May 2017

Inductance Measurement Fixture and Mathematical Model Development to Support AC Drive System Simulation Tools

Garry Jean-Pierre
University of Wisconsin-Milwaukee

INDUCTANCE MEASUREMENT FIXTURE AND MATHEMATICAL MODEL DEVELOPMENT TO SUPPORT AC DRIVE SYSTEM SIMULATION TOOLS

by

Garry Jean-Pierre

A Thesis Submitted in

Partial Fulfillment of the

Requirements for the Degree of

Master of Science

in Engineering

at

The University of Wisconsin-Milwaukee

May 2017

ABSTRACT

INDUCTANCE MEASUREMENT FIXTURE AND MATHEMATICAL MODEL DEVELOPMENT TO SUPPORT AC DRIVE SYSTEM SIMULATION TOOLS

by

Garry Jean-Pierre

The University of Wisconsin-Milwaukee, 2017
Under the Supervision of Doctor Adel Nasiri

Variable frequency drives generate high differential-mode (DM) motor voltages due to the reflected wave phenomenon. The common-mode (CM) voltage produced by a pulse width-modulated inverter changes rapidly, which results in high peak currents to ground. For low-power variable frequency drives in long motor leads application, this can present several issues. Some of these issues include cable charging current, capacitive coupling, DC bus pump-up and failure of the power module due to high instantaneous currents that are usually undetected. In this thesis work, existing drive output filters are used to obtain a mathematical model for the inductors used in these filters. A damping matched resistor cable surge impedance is then added. This method reduces reflections of both DM and CM traveling waves, decreases peak cable charging currents and reduces CM current. Experimental and simulation results are provided to demonstrate the usefulness of the model.

TABLE OF CONTENTS

LIST OF FIGURES

LIST OF TABLES

LIST OF ABBREVIATIONS

CM	Common Mode
dv/dt	Rate of Change of Voltage Over Time
DUT	Device Under Test
EMC	Electromagnetic Compatibility
DM	Differential Mode
HRG	High Resistance to Ground
IGBT	Insulated Gate Bipolar Transistors
PE	Power Equipment
PWM	Modulated Pulse Width
RWR	Reflected Wave Reduction
VFD	Variable Frequency Drives

ACKNOWLEDGMENTS

There are many people I would like to gratefully acknowledge for the role they played in encouraging me through this journey. I would like to express my heartfelt appreciation to my advisory committee: Dr. Adel Nasiri, Dr. Rangarajan M. Tallam, and Dr. David C. Yu. A special thanks to Dr. Nasiri for serving as my advisor and accepting me as part of his power electronics group. A special thanks to Dr. Rangarajan for helping me develop this research topic and for his time, patience, guidance and understanding. A special thanks also to Dr. Yu. It has been an honor to be one of his many students. My gratitude goes to Helen Lewis-Rzezustek for her endless support throughout this work. Thanks to Rockwell Automation for making this study possible by providing all the resources necessary for completing this work. My gratitude also goes to my WisCAMP mentors who have encouraged me in my pursuit of graduate study: Dr. Wilkistar A. Otieno, Dr. John L. Baker, Jr. and Dr. Jian Zhao. I sincerely appreciate all their guidance. Thanks also to some important people who have helped me along this journey: Gigi Pomerantz, Jean Vil, Father Fritz Louis, the Hanzlick family, the Torontow family and the Peironnet family. The most special thanks and appreciation goes to my best friend and wife. Sarah, you gave me your unconditional support and love through all my schooling.

Introduction

I. Background

Several types of inductors are used in alternating current (AC) drive systems, such as direct current (DC) link chokes, three-phase AC reactors, and three-phase reactors with integrated common mode and differential mode impedance. The ability to measure the saturation characteristics and impedance vs. frequency response to create circuit simulation models for AC drive system simulation is vitally important.

II. Objectives

The following are the objectives of this project:

1) Develop circuit simulation models based on measured saturation and impedance vs. frequency characteristics. The modeling method must not require information on inductor geometry, construction and material properties.
2) Demonstrate the usability of the model to typical drive system applications, such as reflected wave, phase current and common mode current.

Chapter One: Background

1.1 Magnetics in Variable Frequency Drives

I. Drives

a. Basic Operation

Variable frequency drives (VFDs) are extensively used in industry to fulfill the need of adjusting the speed control or torque output of AC motors. VFDs utilize modulated pulse width (PWM) to generate an output voltage, current, and frequency that can be changed. When the PWM changes, VFDs create an average output waveform that is a sine wave voltage and a current waveform for which frequency can be varied. Hence, this variable output is used to control motor speed, torque, or position [1]. VFDs permit the speed of a three-phase AC electric motor to be changed each time the behavior of the motor's load changes. When altering its output frequency and voltage, the VFD allows the motor to modify its RPMs to respond to those changes.

b. History with Timeline

Table 1 presents the historical development of drives.

Year	Technology
1886	The birth of the electric variable speed drive system represented by Ward Leonard system
1889	The invention of squirrel cage induction motor
1890	The slip ring induction motor drive – speed control via rotor resistance control
1904	Kramer Drives introduce a DC link between the slip rings and the AC supply
1911	Variable speed system based on induction motor with a commutator on the rotor
1923	Ignitron made controlled rectification possible
1928	The invention of thyratron and grid-controlled mercury arc rectifiers
1930	DC to AC power inversion

1931	AC to AC power conversion by cyclo-converters
1950	Silicon based power switches
1960	Thyristors (SCRs) became available and variable speed drives began
1961	Back-to-back reversing DC drive introduced
1960s	Power semiconductor voltage and current ratings grew and performance characteristics improved
1970	The concept of packaging industrial drives was introduced
1972	First integrated motors with DC converter
1973	Isolated thyristors packages
1970s	The principle of vector control (field-oriented control) evolved
1983	Plastic molding made their first significant impact on VSDs
1985	Direct torque control as a concept
1990	Integrated power modules
1992	A new packaging trend emerged
1996	Universal drives (a general purpose open loop vector drive, a closed loop flux vector drive and a servo drive)
1998	Complete AC/AC integral converter up to 15kW
1998	Medium voltage pulse width modulated voltage source inverter drives – became a commercial product

Table 1. A brief history of the development of VFDs [2]

c. Advantages and Disadvantages

The advantages of using VFDs in modern applications are many. These benefits include improving process control, increasing energy savings, providing higher reliability to the overall system and providing soft-start capability. Soft-start capability reduces the inrush current at motor start-up, thus improving motor performance and reducing stress on the motor. The use of VFDs has also helped to improve the power factors of electrical systems. PWM drives convert the three-phase AC line voltage to a fixed level DC voltage, independent of inverter output speed and power. This conversion, regardless of the power factor of the load machine, helps provide a constant power factor [2].

Despite the advantages of VFDs, some challenges present themselves with their use. VFDs create current and voltage harmonics at the source and on the output side, which can

negatively affect the performance of the motor. The PWM drives are built with fast switching devices that can ultimately cause other problems, such as motor insulation failures, bearing earth current, and electromagnetic compatibility (EMC). In applications where a long transmission line is to be used, traveling wave is another issue that needs to be taken into consideration.

VFDs are by nature very complicated. They consist of multiple advanced electronic devices which in certain applications might be susceptible to disturbances, and thus not provide the desired result. Due to the importance of PWMs in controlling VFDs, a brief summary of how they can affect the performance of the overall system will be presented.

d. Effect of PWM in VFD

PWM is a VFD control method in which a constant DC voltage is applied to recreate an AC-like voltage waveform using power switching devices, such as insulated gate bipolar transistors (IGBTs). In drive applications, IGBTs are known for fast switching, which can cause high dv/dt and voltage overshoot. The rapid rise and fall rate of voltage plus the high peak voltage can result in an anticipated failure of motors. These unfiltered waveforms will greatly impact the life of the motor. The PWM from fast switching devices causes the traveling wave phenomenon, even at short cable distances. This results in motor insulation failure, bearing failure and cable charging current [2]. The high dv/dt and the high voltage induce a non-uniform voltage in the turns of the motor windings. The first few turns get damped, therefore causing insulation failure from phenomena such as partial discharge. High voltage dv/dt causes non-uniform voltage distribution winding failure, which is the differential mode voltage. The common mode voltage generated by the inverter switching, particularly with two-level inverters, appears between the neutral of the motor and chassis. Zero common mode voltage cannot be

generated; it is always a non-zero common mode voltage. Some of this voltage appears on the bearing, therefore cause bearing failure from the dv/dt of voltage and circulating current in the bearing.

PWM also affects the cable that connects the motor to the drive. Shielded cables are used in most VFD applications to contain noise. The consequence of using shielded cables is that the capacitance is high. Therefore, there will be high common mode current that will charge and discharge that capacitance. In the case where shielded cables are not used, there will be a significant EMC issue.

Figures 1 and 2 demonstrate the enormity of voltage overshoot and currents in the leads at each switching of the IGBT. In Figure 1, the voltage on the drive side is in blue and the voltage on motor side in orange. Figure 2 shows the noise spikes and disturbances with nearby components.

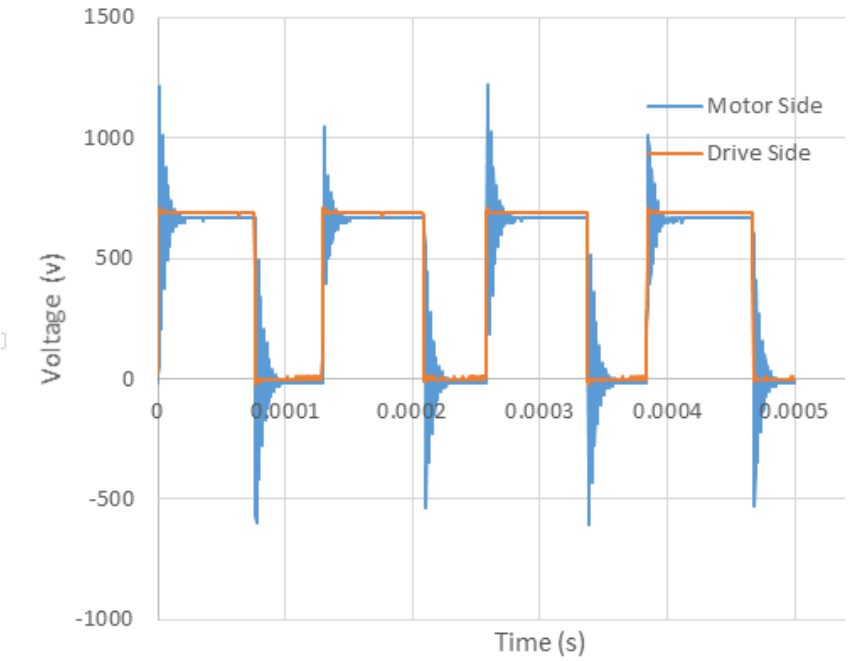

Figure 1. Voltages on the drive and motor sides

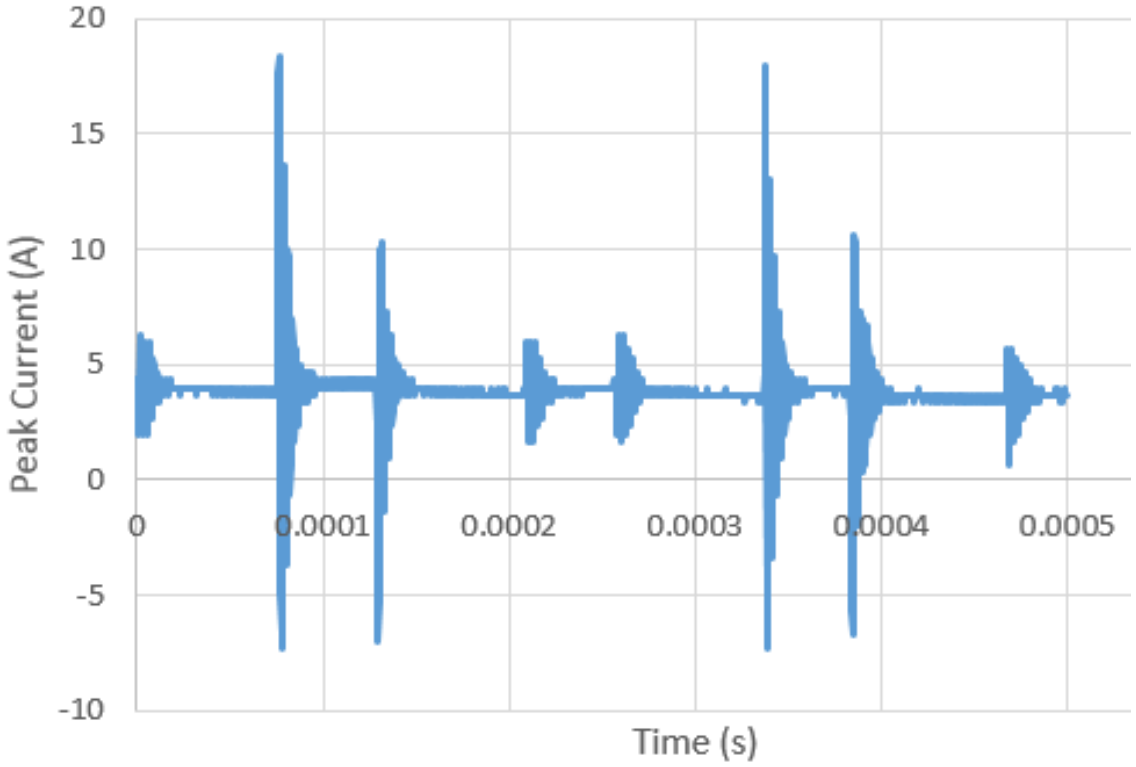

Figure 2. Output phase current spikes and line disturbances

II. Filters

Power electronic switching devices have evolved and become increasingly efficient. This development has enabled high frequency switching operation and improved the performance of PWM inverters for driving induction motors. Figure 3 represents a typical application of a rectifier and a high frequency PWM inverter that controls both the voltage and frequency applied to a motor and, therefore, achieves a variable speed operation over a wide operating range. In many applications, such as fans, pumps, compressors, food processing, water treatment, mining and fracking, PWM inverter controlled induction motor drive applications have been proven to be very successful.

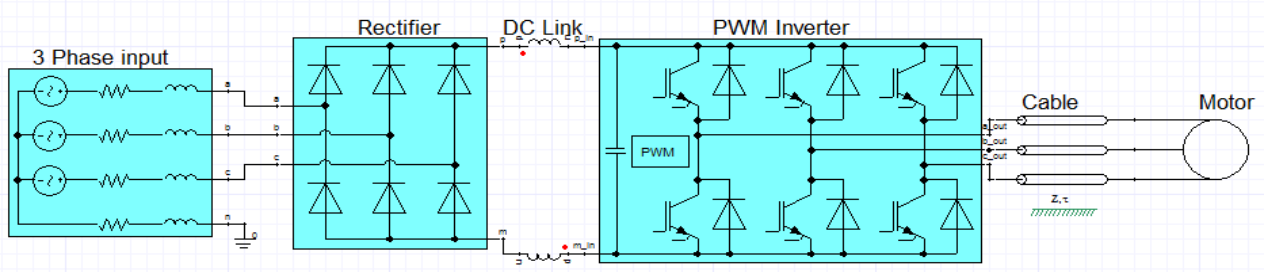

Figure 3. Typical application of a rectifier and a high frequency PWM inverter

In current technology, high switching frequency IGBT use is extremely common. Despite the fact that the performance of PWM in variable speed drives has improved significantly, high voltage rise-up in a short period of time (as seen in Figure 2) may cause uneven distribution of voltages within the motor during switching time and, consequently, cause failure of the motor. In some applications where a long motor cable is used, high frequency noise disturbances on the motor terminals will result in overvoltage, which further stresses the motor insulation.

PWM waveforms can have detrimental consequences on both the motor and the cable. The motor can be affected by the discharge of high frequency and high peak voltage dv/dt, which will cause insulation and shaft bearing failure and possibly create a ground path for current to flow. The cable, particularly when long leads are used, can be affected by the rising and falling edge of the voltage waveform, which creates the voltage doubling effect. As a result of high dv/dt, earth current can flow in the cable stray capacitance [2].

Due to these effects of PWM, many remediated types of filters have been presented. These filters are applied on the terminal side of the inverter in order to mitigate the effects of high frequency noise and excessive overvoltage. They are designed using magnetic components such as inductors, reactors and chokes. In the following section, a brief summary of these magnetics components will be discussed.

1.2 Magnetics Used in Filter Design

I. Inductors

An inductor, commonly named a coil or reactor, is a passive electrical component that stores electrical energy in a magnetic field when current is flowing through it [3]. In filter design, inductors serve multiple purposes: they can control the signal by eliminating noise and only allowing the desired signal to pass, they can store energy and they provide voltage stabilization.

In filter design, the ability to determine the resonant frequency of the inductor is extremely important. Inductors only behave like inductors when below a certain frequency range, commonly named the self-resonant frequency. Above the self-resonant frequency, inductors behave as capacitors. The self-resonant frequency is important because in real world applications, inductors are not completely inductive. They are surrounded by parasitic elements which can affect their behavior. This phenomenon is illustrated in Figure 4 below.

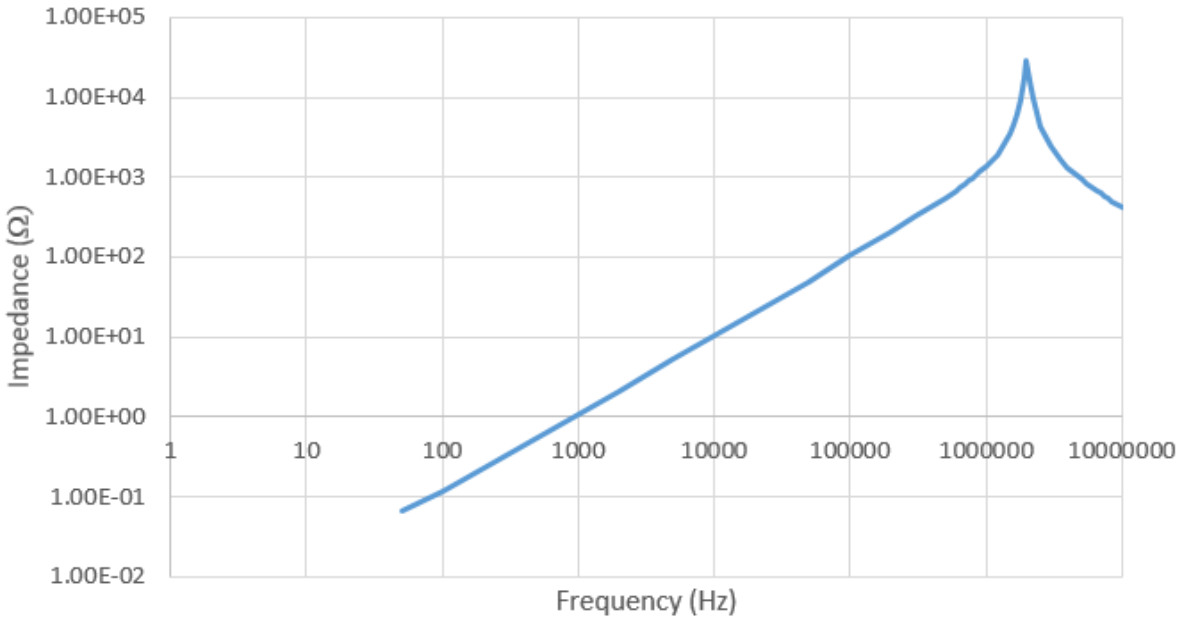

Figure 4. Impedance versus frequency

In a DC circuit application, an inductor helps to limit the rate of change of current in the circuit as the current continuously flows in an inductor. If the applied voltage is increased or decreased quickly, the current is then incremented or reduced slowly. However, when the flow of current changes in the inductor, an equivalent voltage will be created. Consider Equation 1, where V is voltage, L is inductance and di/dt is the rate of change of current in amps per second. When the current rises, a voltage will be created. This induced voltage is proportional to both the rate of rise of current and the inductance value. From this inductance value, one can easily determine the reactance for the reactor in question.

$$V = L\left(\frac{di}{dt}\right) \qquad \text{Equation 1.}$$

II. Line Reactors

Fundamentally, a reactor is an inductor. A reactor is a device comprised of a conductor coiled around a magnetic core, as seen in Figure 5.

Figure 5. Line reactor [4]

When an electric current is applied to the coil, it becomes an electric magnet that has the strength of the field which is proportional to the current flowing and the number of turns, represented by Equation 2. The greater the number of turns, the higher the inductance becomes [5].

$$\emptyset = NI \quad \text{Equation 2.}$$

Changes to current amplitude or direction will be opposed by the existing magnetic field in the core until equilibrium is achieved. In some cases, ferrous material is added as a core to the winding in order to create a better inductor [5].

Drive systems are susceptible to harmonics due to the necessity of AC to DC rectifiers. When the magnitude of the AC line-to-line voltage is greater than the voltage of the DC bus, the drive exclusively draws current. AC line reactors are placed on the input side of the drive and in series with the incoming line. Line reactors help solve the harmonics effects. Due to their location, they are able to act as a buffer for surges and other transients [6].

The reactance is included in the total impedance for an AC circuit. Equation 3 represents the reactance of an inductor. When analyzing Equation 3, one can conclude that the impedance of the reactor is higher with larger inductors. The impedance of a given inductor value increases at higher frequencies. Therefore, one can observe that reactors not only limit the rate of rise in current, but they also add impedance to the system.

$$XL = 2\pi fL \quad \text{Equation 3.}$$

Adding a line reactor between the motor and inverter is not a simple thing. The reactor can add or adjust other resonant modes which are pure transmission line modes and can double the voltage. There are a few disadvantages in using a reactor in VFD applications, such as

increase in the rise time, losses due to wire resistance and eddy current loss in the core due to change in magnetic field and reduction in efficiency. Despite these disadvantages, reactors prove to be important in dealing with harmonics distortion, voltage spike, load inductance effect and reflected wave effect in VFD [2].

On the input side, reactors reduce harmonics. Harmonic compensated line reactors are designed to deal with the harmonic's waveform. Since the current waveform is not a pure sine wave, the current is said to contain harmonics. By injecting an inductive reactance into the circuit, the peaks of the line current are reduced and somewhat broadened out. This makes the current more sinusoidal by lowering the harmonic level.

Not only do line reactors help reduce harmonic distortion when installed in front of the VFD (as seen in Figure 6) they also help protect the drive from most voltage transients. This is done by decreasing the voltage to an amount that is proportional to the current flowing through it. On the incoming power lines, spikes or surges will be reduced when using reactors. When an inductive load is switched off, voltage spike is likely to happen at the input of the drive. As a result, surge current will augment on the input. If the voltage surpasses the rating value, a failure of the semiconductor devices in the DC converter may also happen [5].

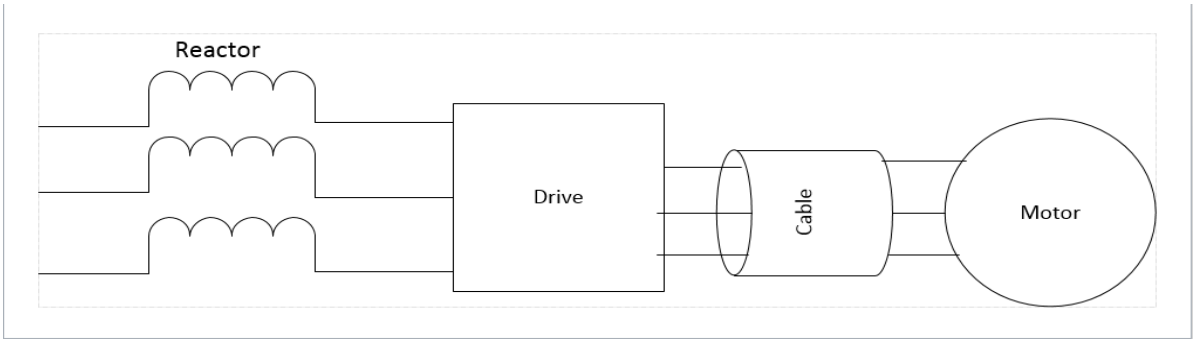

Figure 6. Three-phase line reactors on the input side of the drive

Sometimes, applying a reactor on the output side of the drive is necessary. In the case of a low leakage inductance of the motor, a reactor will help increase the load inductance to a level that matches the drive capability. Therefore, one can say that by inserting a reactor on the output side of a drive, load impedance is added. Reactors also serve as filters by protecting against fast rising voltage pulses dv/dt. Rapidly changing PWM voltage pulses in VFD can affect the inductance and capacitance of long cable motor application. Therefore, peak voltage increases at the motor terminals. The peak overvoltage at the motor terminals increases considerably when a longer the cable is used.

In addition to being used to protect the motor in long motor leads applications, reactors can also be used to reduce the effect of reflected wave. A reactor and a parallel resistor, such as the one in Figure 7, are placed at the output of a drive in order to prevent a reflected wave voltage spike in long motor leads applications. Reactors also help reduce the audible motor noises that are related to the switching of PWM drives. In addition, a load reactor can be used as a current limiting device to protect the drive under motor short-circuit conditions. The line reactor slows down the rate of rise of the short-circuit current and restricts the current to a harmless level [5].

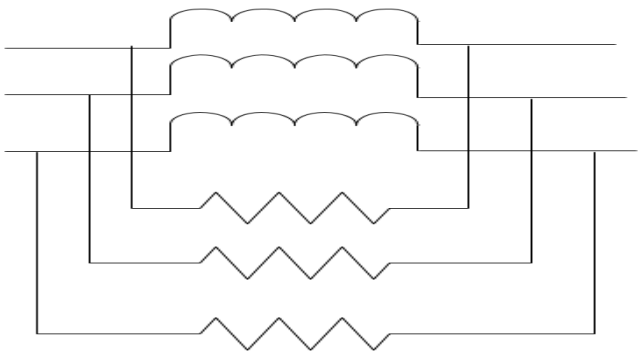

Figure 7. Reactors and resistors placed in parallel

The terms reactor and inductor are often used interchangeably and refer to the same device, although reactance and inductance are not interchangeable terms. At the input of a drive, line reactors protect contra spikes and surges on the power lines, improve semiconductor life, ameliorate the power factor**,** decrease voltage notching, and reduce harmonic distortion. At the output of the drive, in long motor lead applications, load reactors placed between the drive and motor (as in Figure 8) decrease dv/dt and peak voltages at the motor terminals. In addition, they are used to protect the drive from surge currents resulting from fast changes in the load, decrease motor temperature, protect motors from long cable effects, reduce output voltage dv/dt, decrease surge currents, improve semiconductor life and reduce audible motor noise.

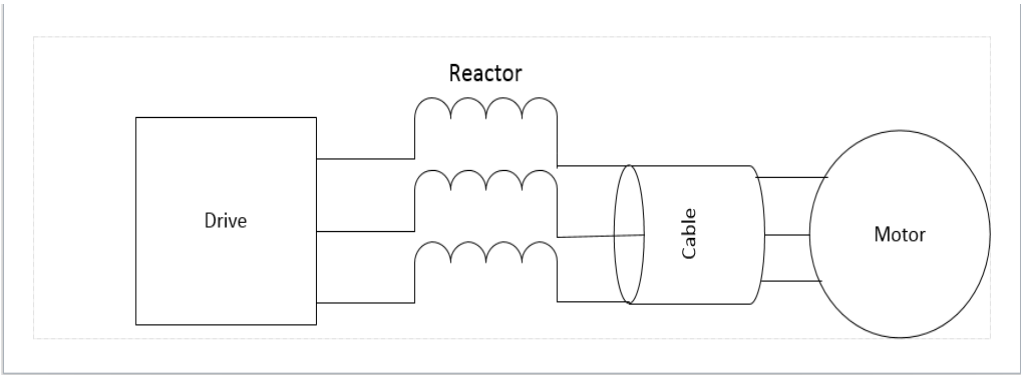

Figure 8. Reactors placed at the output side of the drive

III. DC Link Chokes

In drive design, it is important to pass harmonics testing and to limit the ripple on the bus in order to have good performance. Therefore, filtering is an important part of the design. In general, chokes can be applied either on the DC or on the AC side of the rectifier. Figure 9 depicts a DC choke. The advantage of filtering on the DC side is that the DC link choke consists of only two coils carrying current with no voltage drop. However, on the AC side it gives more immunity to surges as it clamps them before they reach the semiconductor devices.

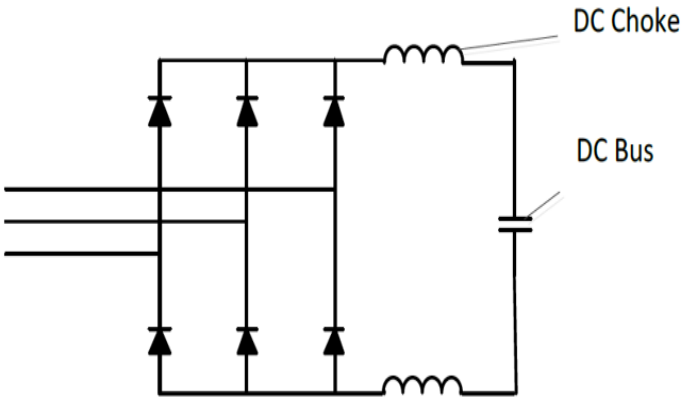

Figure 9. DC choke

A DC link choke reduces harmonics created by the VFD in the same way a line reactor does, but provides less protection against voltage transients. Unlike a line reactor, a DC link choke does not have a current dependent voltage drop.

In summary, chokes placed in series with the internal DC bus in a system will help meet harmonics standards, absorb voltage and current overshoot, reduce AC input line harmonics and decrease AC ripple on the DC bus [2].

1.3 Applications Requirements

In order to completely comprehend the reason why VFDs may cause a faster deterioration of a motor, two phenomena need to be grasped. The first is the reflected wave, or standing wave, phenomenon; the second is voltage overshoot. Theoretically, these two phenomena can be analyzed differently; in real life applications, the solutions remain the same. In this section, issues related to long cable applications and the reflected wave phenomenon will be addressed.

I. Long Cables

In applications where a long cable is to be used on the output of a VFD, many factors must be considered due to the influences of voltage pulses and current harmonics. Reflected voltage waves and current harmonics created with long leads at the motor terminals can have a substantial negative effect on the motor performance if the mitigation of this issue is not being considered accordingly. Consider the fact that in PWM drives, the reflected wave form produces high differential mode (DM) motor voltages. The fast switching of the PWM produces the high peak current to ground, which in turn generates the common mode voltage (CM). These effects can potentially harm the system [7].

There are several electrical characteristic issues that should be considered when using long motor cables in VFD applications. These include cable capacitance, charging current, resistance, voltage drop, current rating and insulation. Cable charging current and capacitive coupling result from switching transitions of the fast rise time of PWM voltages. During switching transition, current spikes travel from line-to-line and line-to-ground in the cable capacitances. High peak cable charging current is a result of all of three phases being switched concurrently at low fundamental output frequency [7].

Consider Figures 10 and 11 for a better understanding of this phenomenon. Figure 10 depicts a three-phase drive connected to a three-phase motor plus a ground cable, where C_{0l} represents the line-to-line capacitance path and C_{og} represents the line-to-ground capacitance path. In addition, there is a motor line-to-ground capacitance, which is defined by the stator winding capacitance.

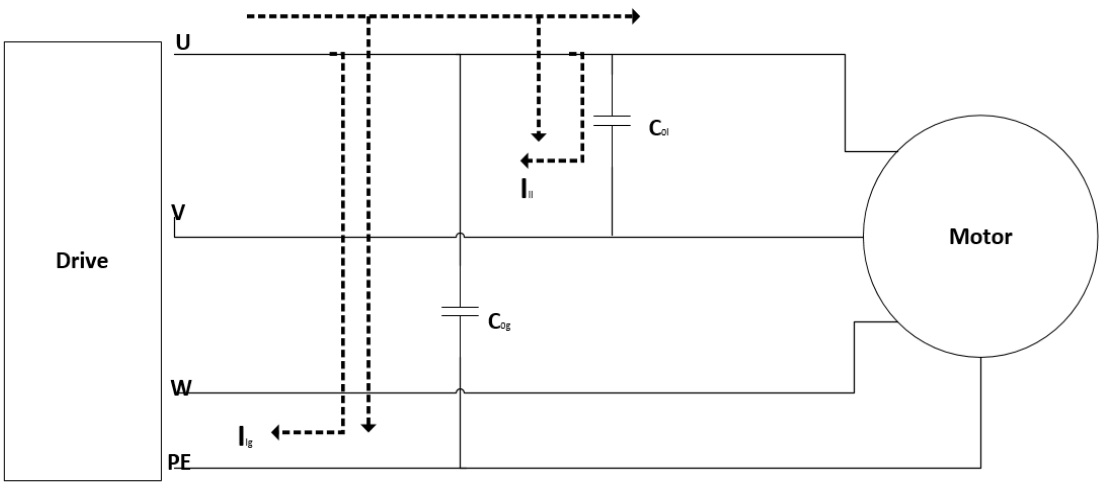

Figure 10. Cable charging current and capacitive coupling phenomenon

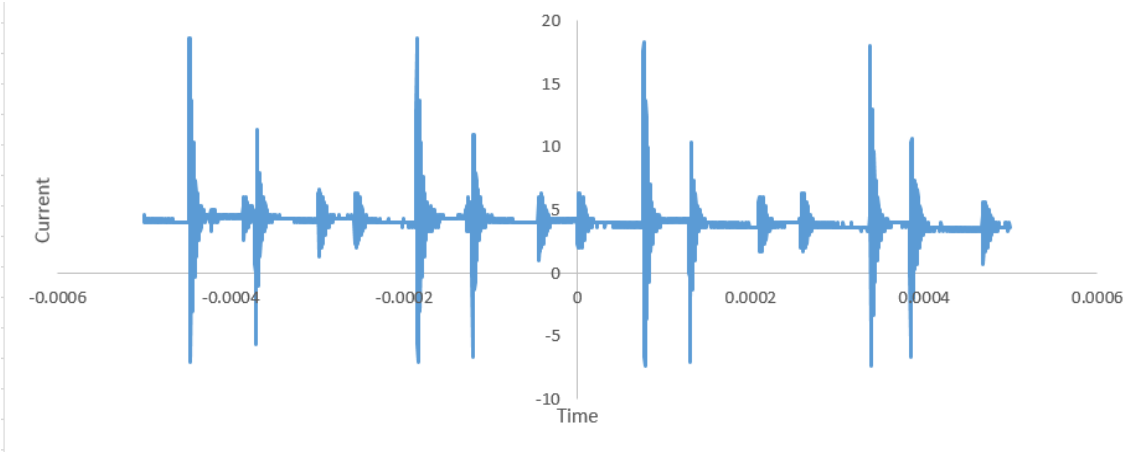

Figure 11. Output phase current through the line

The line current flows through C_{o1} and returns to the drive via another phase. Each IGBT switching transition in a given phase also induces a line-to-ground cable charging current path through C_{og}. [8]. Equations 4 and 5 explain this phenomenon.

$$I_{l1} = C_{01}\left(\frac{dv}{dt}\right) \qquad \text{Equation 4}$$

$$I_{lg} = C_{0g}\left(\frac{dv}{dt}\right) \qquad \text{Equation 5}$$

If the peak current exceeds the instantaneous peak rating of the drive and induced voltages on adjacent cable systems, capacitive coupling and cable charging can consume the drive power. This results in reduced motor torque and drive overcurrent trips. In Figure 11, one can see that at each switching instant, the peak current reaches about 20A. Nearby communication between the long cable and other cables or devices can cause the generation of noise sparks each time the IGBT switches. It is also known that the phase-to-ground and phase-to-phase capacitance increases with the amount of lead length used. Therefore, it is possible for an overcurrent fault to occur during the time that the inrush current is charging the line-to-line and line-to-ground capacitance. These types of issues are more frequent in low power drive applications and can be prevented by using proper filtering techniques.

Another common issue with long lead motor cables is the DC bus voltage pump-up. Based on the grounding system, at light or no load and low speed, this issue may surface. This usually happens when the common mode current flows back to the cable shield and the ground path to the DC bus capacitor of the VFD [9]. As seen in Figure 12, the path followed by the ground current is a low impedance path due to the AC inputs of the system being tied together at the downstream ground source.

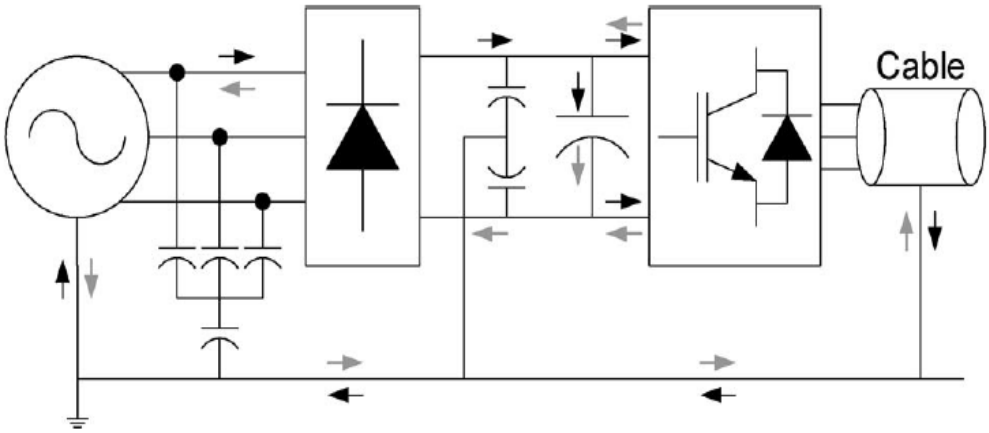

Figure 12. Illustration of the DC bus pump up phenomenon

The common mode current has the highest amplitude at a lower output frequency because most of the switching of all the phases happens at the same time. However, in long cable applications at high PWM frequencies, DC bus pump-up further degrades [7].

II. Reflected Wave Reduction (RWR)

The inverter segment of a drive does not generate a sine wave output voltage, but instead produces a string of interminable voltage pulses created from the DC bus. These voltage pulses travel back and forth through the motor cables to the motor and then reflect back to the drive [10]. These waveform images are a function of the rise time of the drive output voltage dv/dt, cable characteristics, cable length and motor impedance. Mismatch in impedance allows voltage pulses to be reflected back in the same direction from which they were generated. As these reflected waves come across incoming waves, their values add and produce higher peak voltages. As the overshoot peak voltage increases proportionally to the wire length or the carrier frequency, the motor insulation degrades and fails [10]. This phenomenon is commonly known as the reflected wave phenomenon.

Figure 13 provides a clearer picture of the voltage overshoot problem. The Figure presents two graphs. The orange graph is the PWM waveform at the output of the drive. The blue graph is the PWM waveform on the motor side. The overshoot in the blue graph is a function of the energy stored in the leads during the rise time of each output voltage pulse dv/dt. Knowing that the inductance is a function of the cable length between the motor and the drive, one can say that the inductance increases the amount of time it takes to charge the capacitance of the motor. This in turn augments the amount of energy in the cable. At the time the motor reaches the right voltage level, the remaining energy in the cable continues to charge the motor

voltage, therefore generating voltage overshoot. In fact, in cases where the cable is long enough, the motor terminals may see up to twice the DC voltage of the VFD, as one can see in Figure 13. The conclusion can be drawn that the greater the distance between the motor and the VFD, the more voltage overshoot will occur.

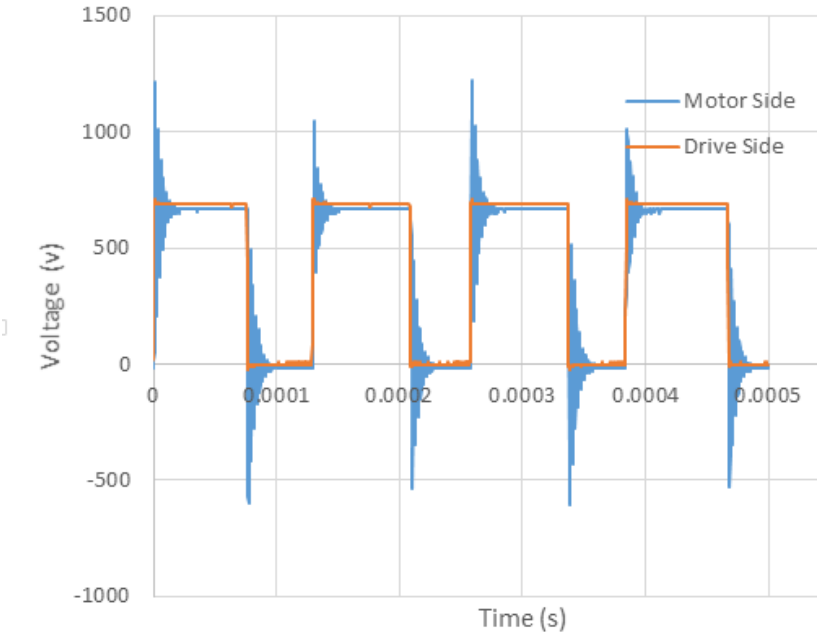

Figure 13. Voltages on the drive and the motor sides

Reflected wave voltage is a common problem in VFDs with longer motor leads. A mismatch between the motor impedance and the cable creates a reflected voltage at the location where the leads are attached to the motor windings. This reflected voltage creates a standing wave phenomenon and can potentially double the voltage at the motor terminal. Higher voltages increase the probability of motor and drive failures. The reflected wave phenomenon can be explained using the transmission lines theory, as represented in Figures 14 and 15. The two-wire line is shown with one phase and neutral return path, where L and C represent the inductance and capacitance of the line.

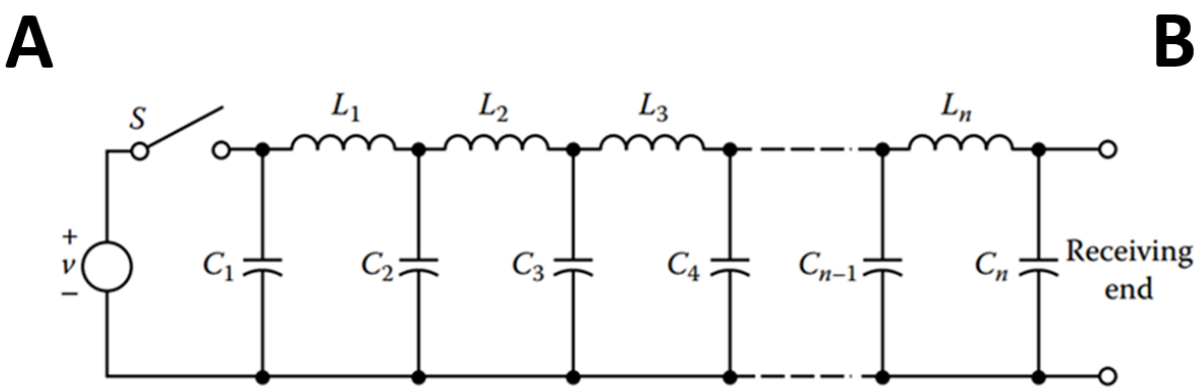

Figure 14. Lumpy representation of a transmission line [11]

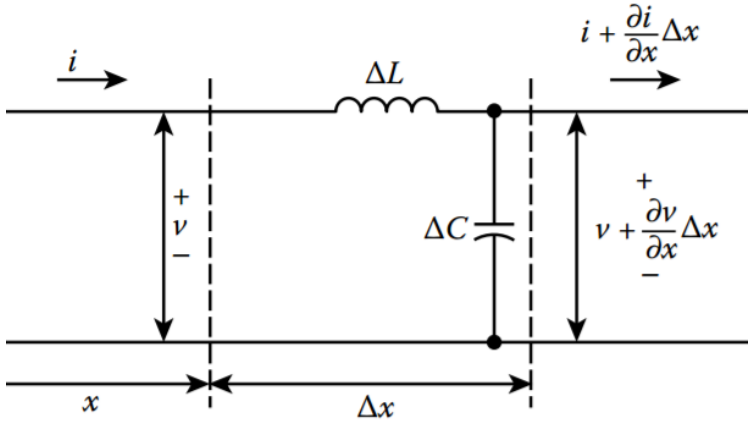

Figure 15. A segment of the elements from Figure 14 [11]

From Figure 14, consider the case when a voltage source is applied and the line is suddenly connected via the closing of the switch. The line is not energized from point A to point B instantaneously. When the source voltage is applied, C1 is charged immediately. However, because of the first inductor, the second capacitor does not charge immediately. The same phenomenon is also true for the other capacitors. Thus, the capacitor at point B will see a greater delay. This bit-by-bit increase of voltage over the transmission line conductors can be viewed as a voltage wave traveling from A to B and vice versa. The gradual charging of the capacitances is due to the associated current wave [11].

In the case of mismatch, the wave might take infinite round-trips from the drive to the motor. For the purpose of analyzing the line termination in impedance, let V^+ represent the forward wave reflection, which is the forward complex amplitude, and V^- represent the backward reflection wave, which is the backward complex amplitude. The ratio between these two complex amplitudes gives rise to the voltage reflection coefficient r, which is defined in the following equations, where Z_c is the characteristic impedance of the cable and Z_L is the load impedance [12].

$$V^+ = \frac{I_L}{2}(Z_L + Z_c)^{\gamma l} \qquad \text{Equation 6}$$

$$V^- = \frac{I_L}{2}(Z_L - Z_c)^{-\gamma l} \qquad \text{Equation 7}$$

$$r = \frac{Z_L - Z_c}{Z_L + Z_c} \qquad \text{Equation 8}$$

The Bewley Lattice Diagram, as shown in Figure 16, is an extremely useful tool to keep track of traveling voltage or current wave as it reflects back and forth from the ends of the line.

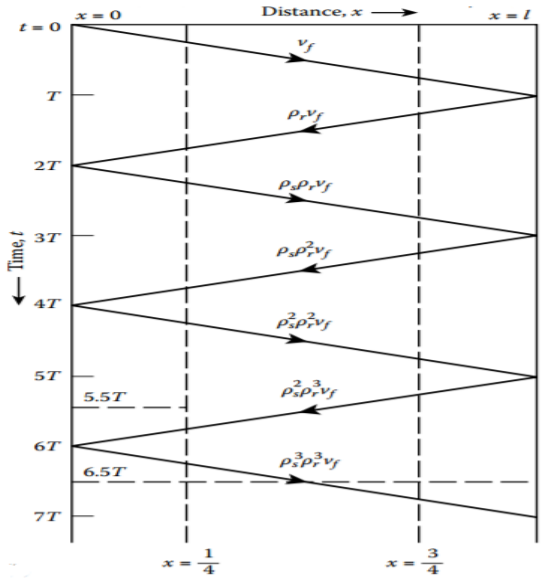

Figure 16. Bewley Lattice Diagram [11]

Figure 17 shows the circuit diagram that is used to determine the proper equation for the lattice diagram, where Z_s and Z_L represent internal source impedance and the load impedance, respectively. In the lattice diagram, the horizontal line is the distance between the sending and receiving ends and the two vertical lines represent the time (T). The diagonal zigzag line represents the wave as it travels back and forth between the ends or discontinuities. The slopes of the zigzag lines give the times corresponding to the distances traveled.

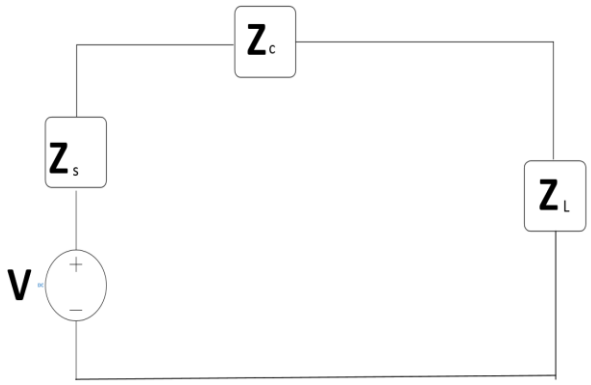

Figure 17. Circuit that represents the impedance of the lattice diagram

The reflection waves are found by multiplying the incident waves by the corresponding reflection coefficient. The voltage at a given point in time and distance is calculated by adding all terms that are directly above that point [11].

At the output side of the drive in long motor cable applications, an RWR device placed between the motor and the drive helps decrease dv/dt and peak voltages at the motor terminal. Figure 18 shows the configuration of an AC drive, RWR, cable and motor. Due to the fast changes in the load, the use of an RWR device will preserve the drive from the effect of surge currents. For IGBT drive applications with long lead lengths from the motor to the drive, RWR devices can help protect against fast dv/dt rise times. In summary, RWR will assist with

protecting motors from long lead effects, decreasing surge currents, reducing output voltage dv/dt, improving semiconductor life, reducing motor temperature and decreasing audible motor noise [13].

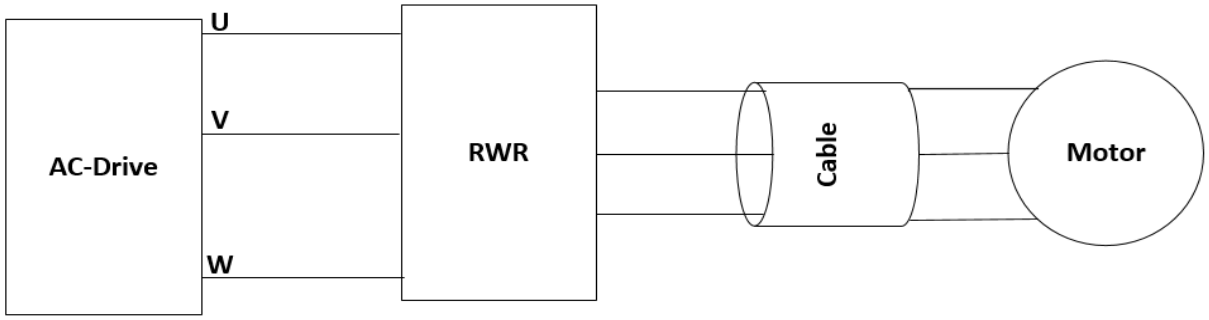

Figure 18. Configuration of an RWR device

Chapter 2: Prior Art and Limitations

2.1 Prior Art

Many papers have proposed possible methods for overcoming the issues of voltage overshoot and common mode noise in long leads motor application. Solutions from previous research to these issues can be categorized into three main groups: passive filters (represented by Figure 19) resonant inverters (as seen in Figure 20) and inverter output filters (as depicted in Figure 21). In this section, a few of the RLC filters that have been presented to mitigate these issues and their limitations will be presented.

I. Passive RLC Filters

An inverter output low-pass filter, as seen in Figure 19, was proposed in order to eradicate the effects of long motor leads in VFD applications. This RLC filter is comprised of a damping resistor in series with a capacitor in order to match the surge impedance of the cable. This would provide the proper level of damping to control the voltage overshoot. The design had the goal of reducing the dv/dt of the inverter output pulses below the critical value, such that over voltages would not occur at the end of long cable motor terminals [14].

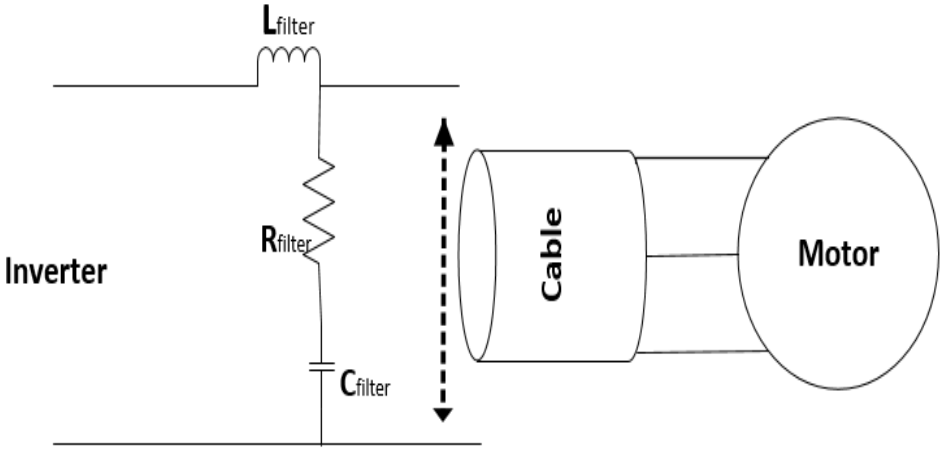

Figure 19. A typical passive LRC filter

II. Series of Filters to Mitigate Both CM and DM dv/dt

EPCOS introduced an output filter configuration for PWM drive systems which was proven in their experiment to reduce both differential and common mode dv/dt at the motor terminals, even in the presence of long motor cable leads. Their method consisted of an LC circuit, as shown in Figure 20. This method depicts two series of filters added together with the objectives of creating a near sinusoidal differential mode voltage in the application of long motor leads and reducing the dv/dt of common mode voltage, consequently reducing the peak cable charging [15].

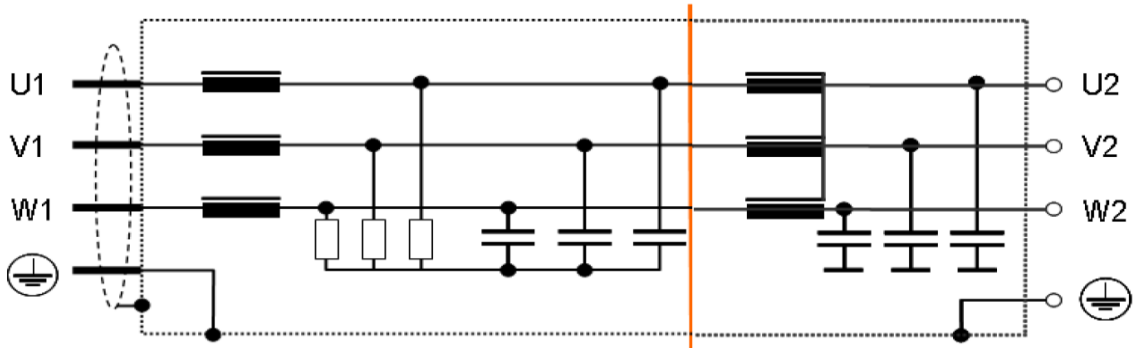

Figure 20. Series of filters to mitigate both CM and DM dv/dt [15]

III. LRC Network Electrically Connected to the DC Midpoint

Another output filter was proposed for VFD systems with the same goal of reducing both differential and common mode dv/dt. The proposed filter consists of a three-phase LRC network electrically connected to the DC midpoint, as shown in Figure 21. In this filter, the midpoint '0' represents the voltage at the DC-link which is a low dv/dt. The voltage between the motor terminal and the ground is the common mode voltage across the filter RC network. As a result, the overall voltage between the motor terminal and the ground is a low dv/dt. The differential mode dv/dt is then decreased due to the RLC network [16].

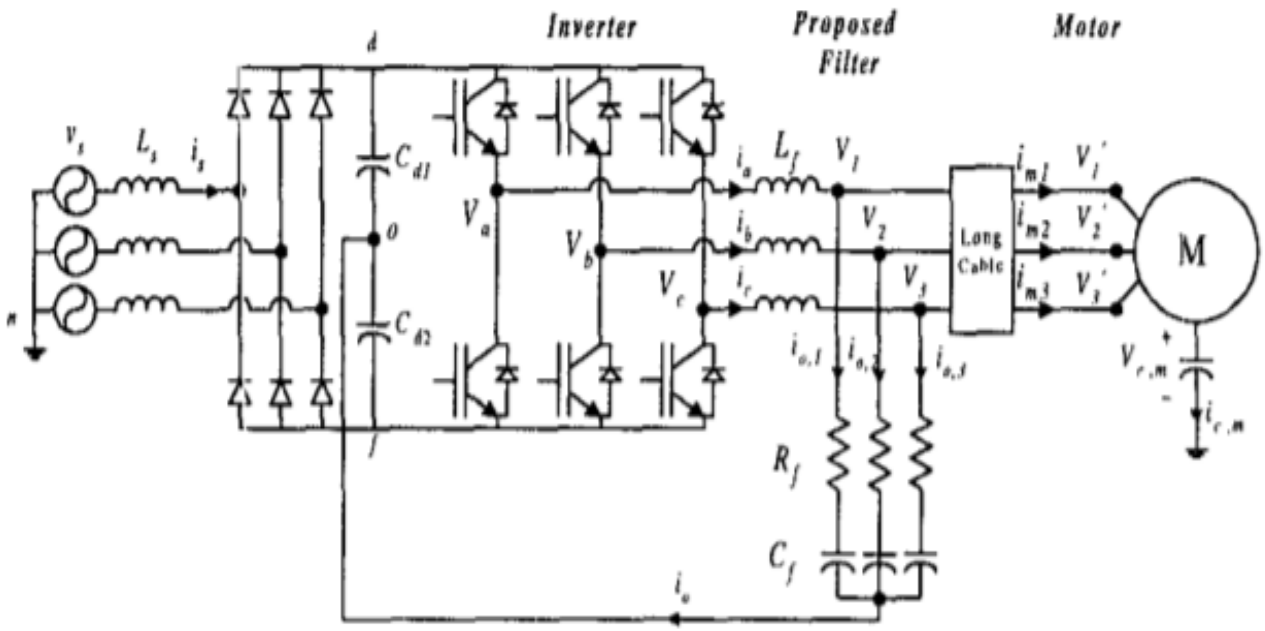

Figure 21. LRC network electrically connected to the DC midpoint [16]

IV. Resonant Filter With Diodes Clamp

Another implementation of an RLC filter, as shown in Figure 22, has been utilized to reduce the rate of rise of the inverter output voltage and to scale down the common mode noise to the motor. This configuration includes diodes to clamp the resonant voltage as the switching frequency is below the resonant frequency of the filter. The theory of operation of this design can be explained using only one of the phases, since they are independent of each other. When one of the switches is on, the corresponding capacitor charges at the resonant frequency until it reaches the bus voltage while the current in the inductor increases. At this point, the clamping diode clamps the voltage. In the event where the voltage is clamped, the current in the inductor decreases according to the voltage drops across the other passive devices [17].

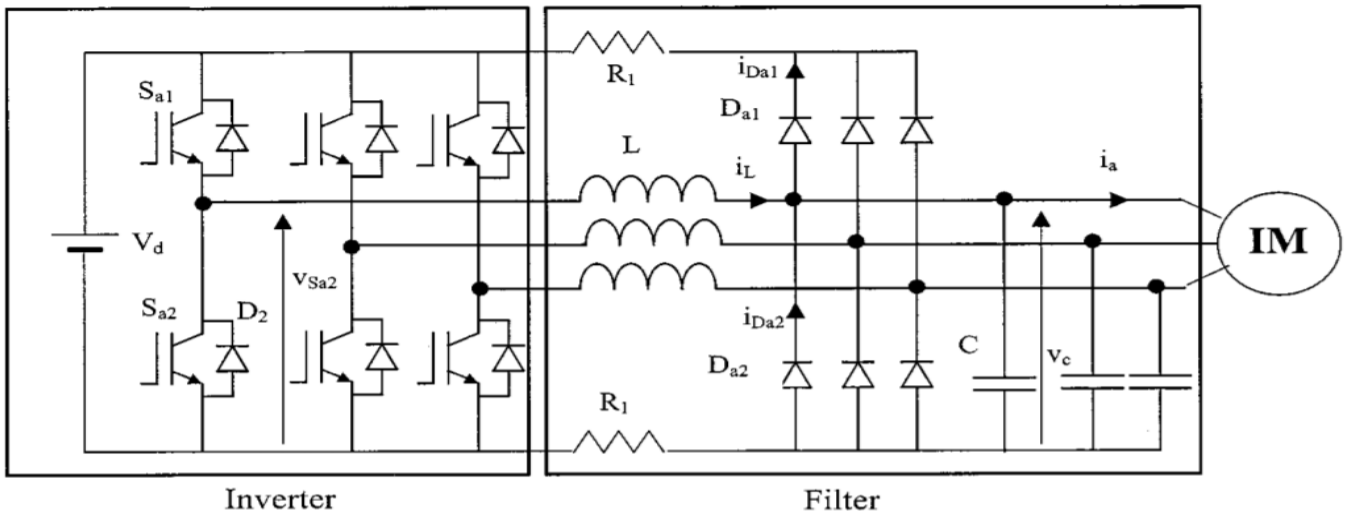

Figure 22. Resonant filter with diodes clamp [17]

V. LR Filter Plus Common Mode Core

Figure 23 represents another drive output filtering method which is used to solve the problem of the differential mode reflected wave phenomenon. In this implementation, a common mode core is placed before the three-phase reactor connected in parallel with the damping resistors. The overall goals of this system are to provide insignificant common mode impedance, limit the peak motor voltage, eliminate reflections and reduce the ring-up of motor voltage [18].

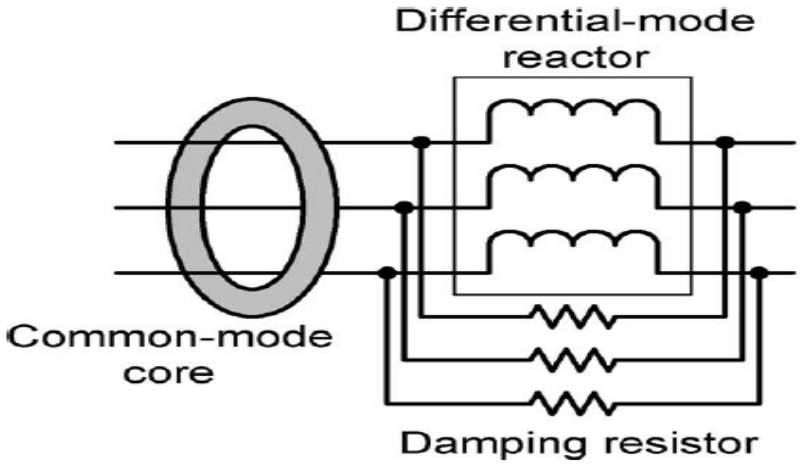

Figure 23. LR filter plus CM core [18]

2.2 Limitations

Several methods to reduce dv/dt and to eliminate the reflected wave have been proposed. However, each of these solutions has their own drawbacks and have been ineffective in completely solving the problem. In the first presented method, shown in Figure 19, the filter did not address both the differential mode and common mode. In the second method, seen in Figure 20, the filter presents a low impedance to ground for low-frequency CM voltages. In the third implementation, presented in Figure 21, the filter reduces the peak CM voltage at the motor terminals. Its effect on CM currents, which is the main issue for low-power drives, was not taken into consideration. The next output filter with the diode clamping, shown in Figure 22, prevents output voltage ring-up and reduces dv/dt, but its approach on common mode voltage and cable charging current were not presented. The final method, seen in Figure 23, can provide good differential mode impedance. However, it is insufficient to address the common mode issues.

Besides the above mentioned issues which previous works did not address, when implementing a combined common mode and differential mode filter to mitigate the effects of fast rise dv/dt and the reflected wave phenomenon, other problems can occur. Problems with saturation alone, three-phase versus one-line simulation, saturation plus coupling and inductance variation when DC bias current is applied at high frequency can be very cumbersome.

I. Saturation

In theory, inductors are idealized so a mathematical model can be used for the analysis. An ideal inductor has inductance, but does not have resistance or capacitance. However, in real life applications, real inductors have side effects which will result in the change of properties and behaviors. They have resistance, due to the resistance of the wire and energy losses in core

material, and parasitic capacitance, due to the electric field between the turns of the wires. Depending on the type of inductor, at high frequencies the capacitance can begin to affect the inductor's behavior. At some frequencies, real inductors behave as resonant circuits. Above the resonant frequency, the capacitive reactance X_c, as seen in Equation 9, becomes the dominant part of the impedance of the circuit. When the frequency increases, the resistive losses in the windings increase due to skin effect and proximity effect [19].

$$Xc = \frac{1}{wC} = \frac{1}{2\pi f C} \qquad \text{Equation 9}$$

The green curve in Figure 24 illustrates the saturation phenomena of an inductor.

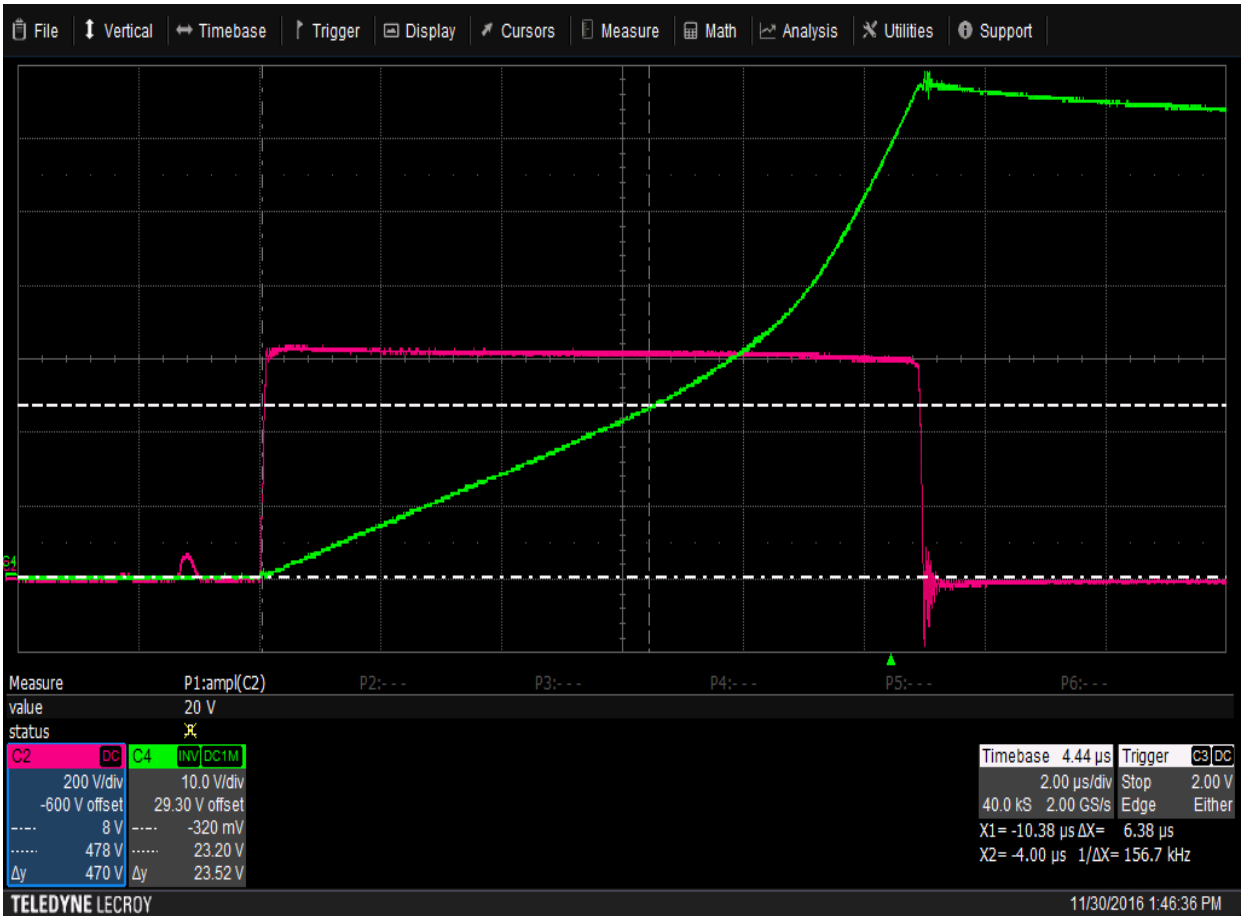

Figure 24. Saturation curve

In Figure 24, one can see that at the beginning of the green curve, the magnetic flux *B*, the current *I*, and the magnetic field intensity *H* are all zero. Increasing the current in the inductor results in applying the field with intensity *H* according to Ampere's law. This curve can be divided into three regions. The first region corresponds to reversible domain wall displacements. In the second section of the curve, the induction *B* increases much faster until it reaches the peak current value with the increase of *H*. The third section of the saturation curve is flat, because the level of *H* is already much greater than the two previous sections. The inductor reaches saturation and a further increase in *H* results in a very small increase in B. The maximum value of *B*, the saturation induction value B*sat*, is practically reached. Thus, this curve is vital in determining at what current level the inductor will saturate.

The magnetic core saturates when the current that passes through the coil is high enough. In this case, the inductance value will change with respect to the current through the device. Increase in flux density is not a simple linear effect. At higher currents, the increase is faster until it reaches saturation. Past the saturation point, the change can be characterized as linear. Changes in inductance are not preferred, as they can have many side effects on the design. Filter designs for drive application saturation should be especially avoided. Therefore, special consideration should be given to saturation in an inductor model for filter design.

II. Three-Phase Versus One-Line Simulation

While the basic traveling-wave equations stays the same when a three-phase system is taken into consideration, mutual coupling exists between the phases of the system and must be part of any calculation. In single-phase applications, it is possible that line losses attenuate and delay the traveling voltage wave along the line. However, in three-phase applications, the situation is much more complicated due to the mutual coupling existence between the phases,

which induces second-order changes of voltage on each phase to be functions of the voltages on the other conductors [11].

2.3 Common Mode (CM) Versus Differential Mode (DM)

Being able to establish the difference between CM and DM noises is vitally important for a better understanding of how noise propagates within a system. CM current is defined as the sum of the current in all three phases on the output side of the drive. CM voltages are created by shaft voltages and circulating leakage currents via parasitic capacitance between motor windings, rotor and frame [20]. CM voltage happens at the time when the voltages on the three output lines of the drive do not add up spontaneously to zero [21]. It is the unwanted signal of a system. Conversely, DM signal is the signal on the two lines of a closed loop with the current flowing in the opposite directions. This type of signal essentially appears in series with the desired signal [22].

The rapid change of the dv/dt output voltage of drives' IGBT creates the possibility for the CM electrical noise to increase. CM noise is a type of electrical noise generated on signals with respect to ground, as seen in Figure 25 below [13]. The CM voltage generated by the PWM drive creates CM currents that travel via parasitic capacitances found in the motor and the cable, as also seen in Figure 25. This points out the path of CM parasitic capacitances in the cable from each line to ground through the shield and ground wire. Figure 25 also shows the locations of the CM parasitic capacitances in the motor from the frame through the motor bearings to ground. The gray lines with the arrows highlight the paths followed by the CM current.

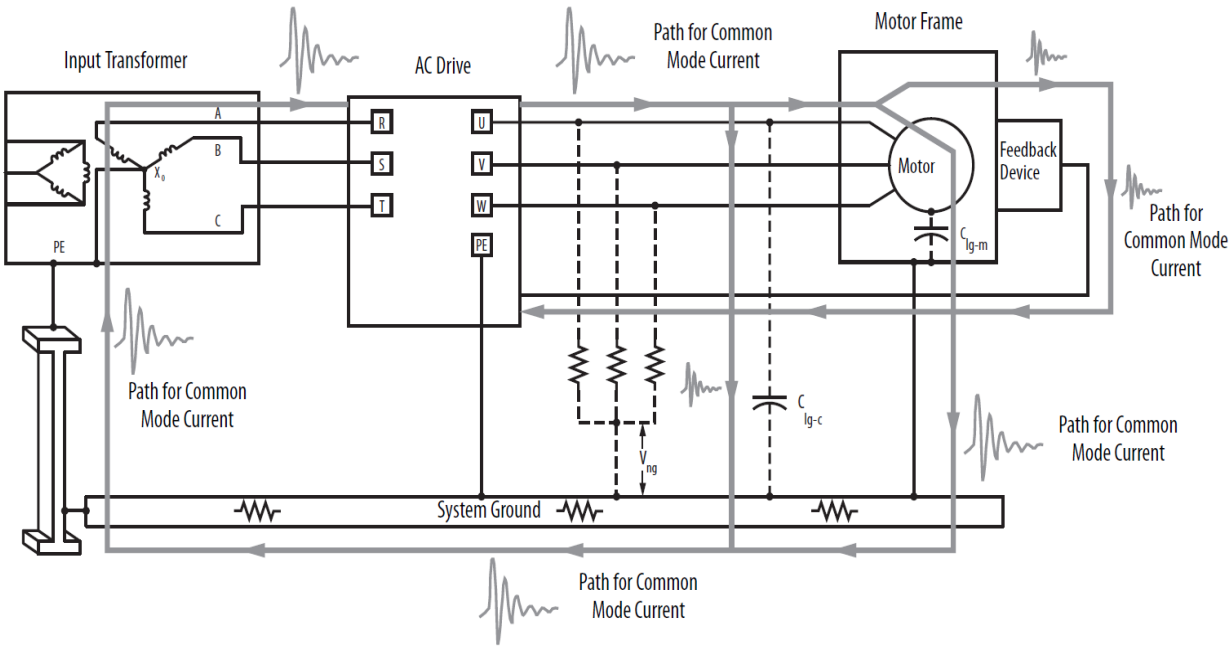

Figure 25. Common mode current path [13]

I. Effect of DM Signal on a Coupled Inductor

Consider Figure 26 below. Assume current I_1 flows from p_1 to n_1 and I_2 flows from n_2 to p_2. The DM current is circulating in opposite directions through the windings. It induces a magnetic field with the same magnitude but with opposite direction, therefore cancelling each other out. This results in zero impedance in the choke to the DM signal.

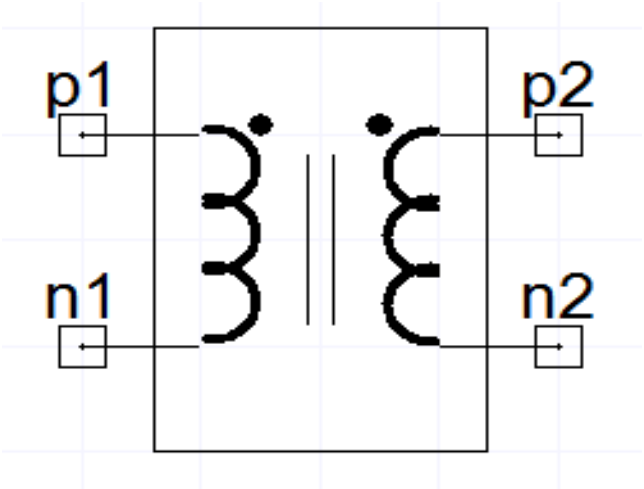

Figure 26. Differential mode coupled inductor

II. Effect of CM Signal on a Coupled Inductor

Consider another scenario in Figure 26 above. This time current I_1 flows from p_1 to n_1 and I_2 flows from p_2 to n_2. The CM current is circulating in the same direction in the windings. It induces a magnetic field with the same magnitude, which add together, therefore presenting a high impedance to the common mode signal [22].

In summary, CM noise is the electrical noise signal on all three lines with respect to ground. DM noise is the electrical noise signal between one phase with respect to another phase. When considering a filter for use in a VFD application, it is important to emphasize that CM noise reduction is an extremely important factor as VFDs produce less DM signal due to the existence of DC bus capacitors.

2.4 The Filter Model

As previously stated, variable frequency drives create high DM voltages at the motor terminals. In addition, the CM voltage generates high peak current due to fast transition. In applications where long cable motor leads are necessary, filtering is extremely important in order to mitigate these issues.

With the objectives of damping the oscillations resulting from reflected wave phenomenon and reducing the peak CM current at the drive output and the peak voltage on the motor side, this filter model will help provide impedance to the CM with damping equal to the cable characteristic CM impedance. Simulation results can be found in chapter 4. In this model, the parameters are:

R_s = series resistance

R_p = parallel resistance

L_p = parallel inductance (which also represents the tested inductor)

R_w = winding resistance

C_w = winding capacitance

K = coupling

L_s = series inductance

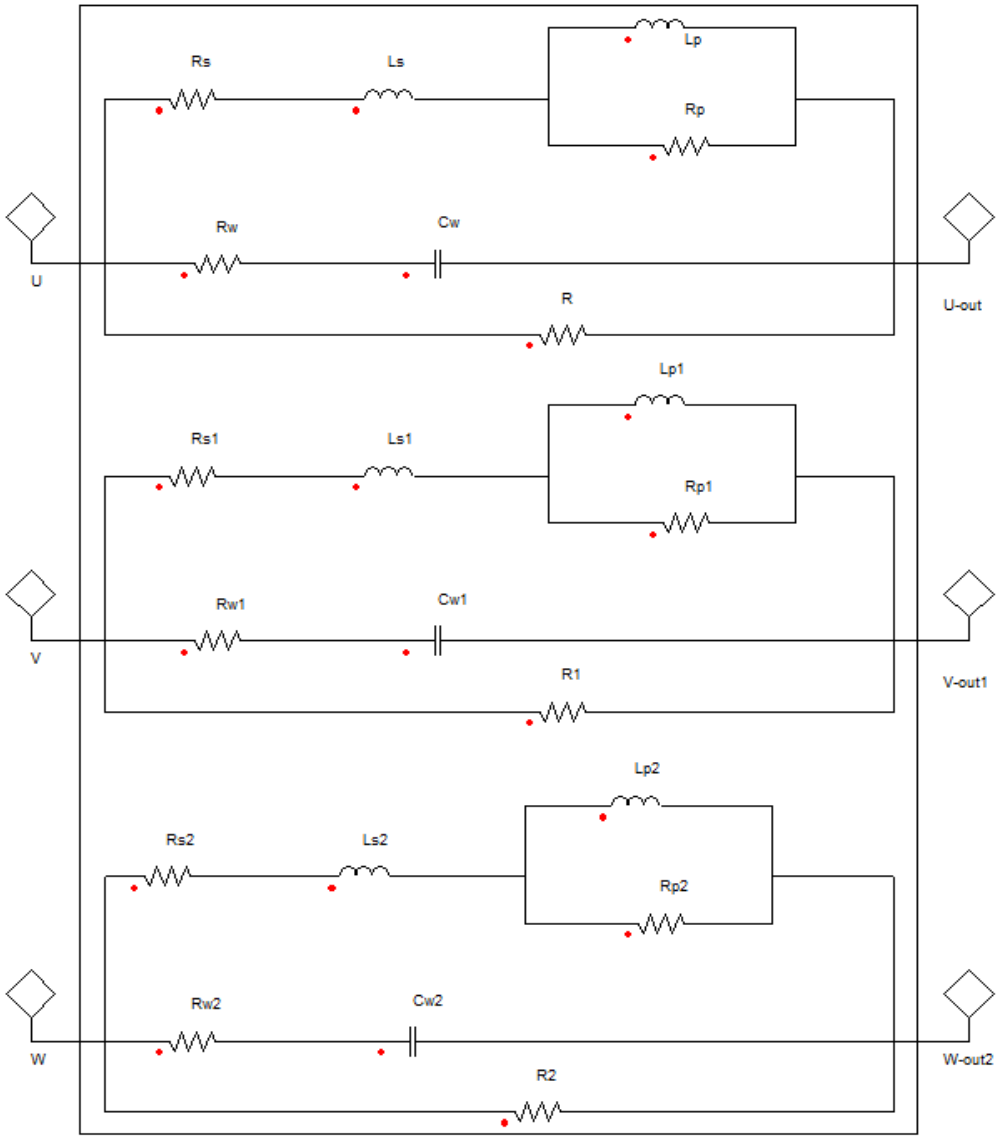

Figure 27. Filter model

Chapter 3 - Contribution and Construction

3.1 Contribution

In this chapter, a new drive filter topology is presented, which has integrated DM and CM impedance with parallel resistance. This method will have the potential of eliminating the reflections of traveling waves and consequently reducing peak line-to-line and line-to-ground cable charging currents and peak CM current. This topology is a generic approach to model single-phase and poly-phase inductors with coupling, with the exception that the modeling method must not require information on inductor geometry, construction or material properties.

The objectives for this project include:

1) Develop circuit simulation models based on measured saturation and impedance vs. frequency characteristics. The modeling method must not require information on inductor geometry, construction or material properties.
2) Demonstrate the usability of the model to typical drive system applications such as reflected wave and common-mode current.

3.2 Constructions

Two types of testing methods were conducted on a single-phase inductor, a three-phase inductor and a common mode inductor in order to model the filter. For each component, single pulse test and frequency versus inductance with and without bias were measured at different levels and configurations, which will be presented in detail in the following paragraphs.

I. Pulse Inductance Test or di/dt Test

This test method is mainly used for testing inductors at high currents. During this test, a rectangular voltage is applied to the device under test (DUT) for a period of time and a pulse is

then sent to the drive in order to generate a current waveform. From this, the inductance of the inductor at different current levels can be calculated. In this method, when DM (CM) is measured, there is no CM (DM) excitation. Figure 28 shows the configuration for a single pulse test.

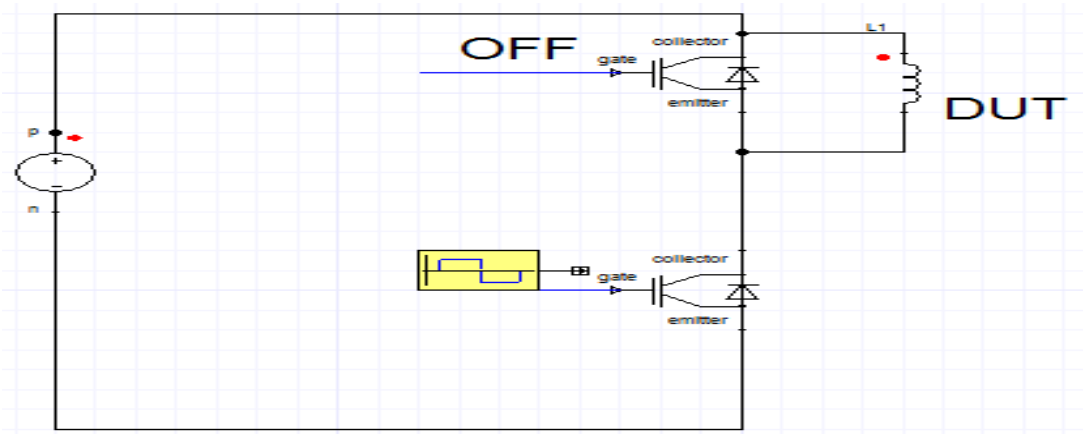

Figure 28 Single pulse test configuration

a. Single-Phase Inductor

In the first measurement set-up, a single pulse test was performed on a 9A, 180uH inductor (as seen Figure 29) connected across the upper phase on the output of the drive. The set up contained a high voltage DC power supply, a frame 2 Allen Bradley drive, a pulse box, a current sensor, voltage probes, the DUT and an oscilloscope.

Figure 29. Single-phase inductor

By sending a pulse to the upper phase of the IGBT, the waveforms in Figure 30, which represent the saturation characteristic for either DM or CM, were generated. From the current curve, the inductance of the inductor was calculated for different current levels over a period of time in order to determine the behavior of the inductor. Results of the calculations are shown in Table 2. The behavior of the apparent inductance and the estimated Lambda are shown in Figures 31 and 32, respectively.

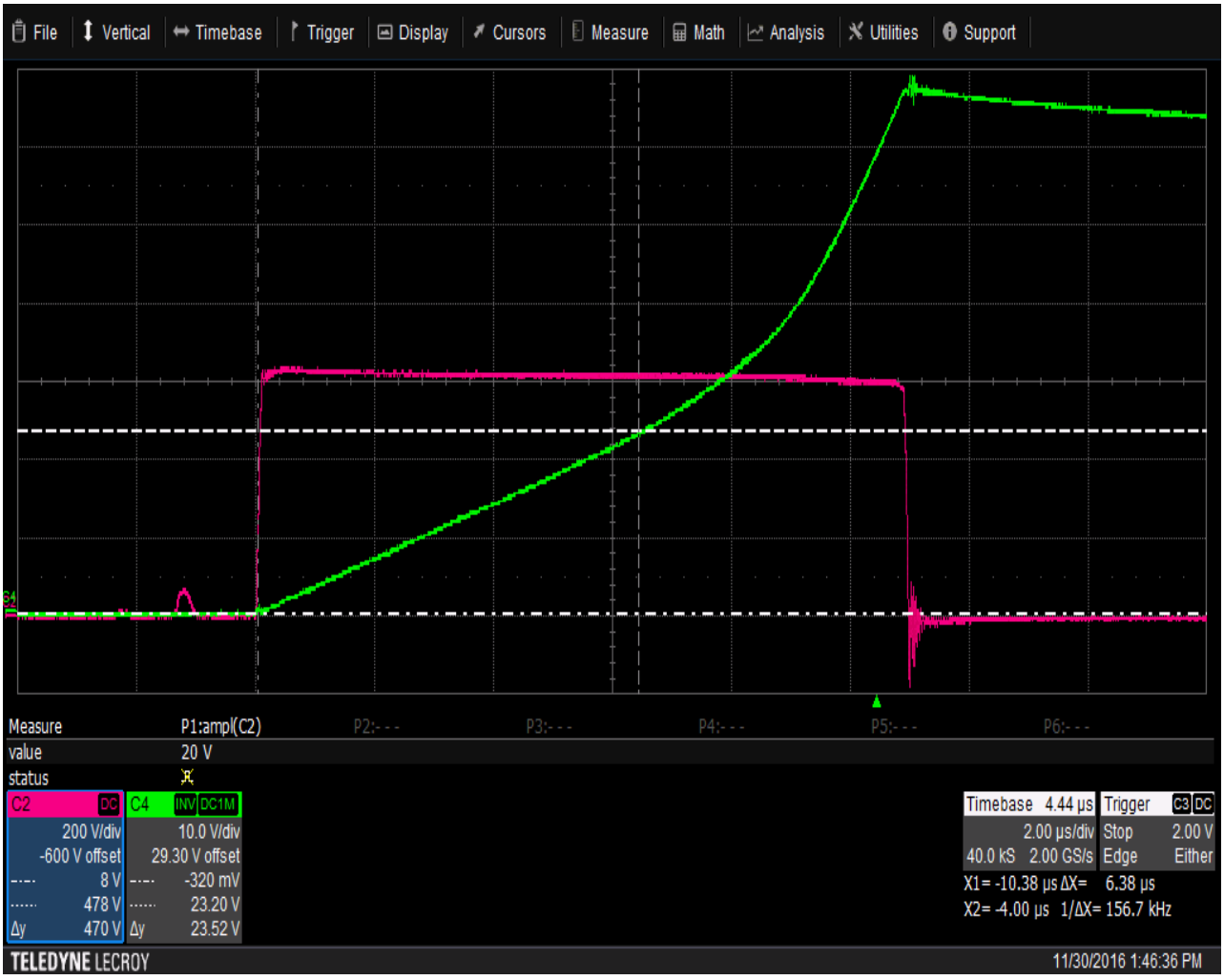

Figure 30. Saturation characteristic curve for the single-phase inductor

I_1	I_2	I_{ave}	ΔI	Δt	V_{ave}	Λ	L
		0				0	1.80E-04
7.7	14.2	10.95	6.5	2.00E-06	600	0.00202154	1.85E-04
18.6	21.4	20	2.8	8.00E-07	600	0.00363264	1.71E-04
20	23	21.5	3	8.00E-07	600	0.00388121	1.60E-04
21.4	24.9	23.15	3.5	8.00E-07	600	0.00412635	1.37E-04
27	30.9	28.95	3.9	8.00E-07	600	0.00488099	1.23E-04
30.9	33	31.95	2.1	4.00E-07	600	0.00523703	1.14E-04
33	36.5	34.75	3.5	4.00E-07	600	0.00549303	6.86E-05
36.5	40.5	38.5	4	4.00E-07	600	0.0057341	6.00E-05
60	67	63.5	7	4.00E-07	600	0.00691268	3.43E-05

Table 2. Saturation characteristic results for either DM or CM

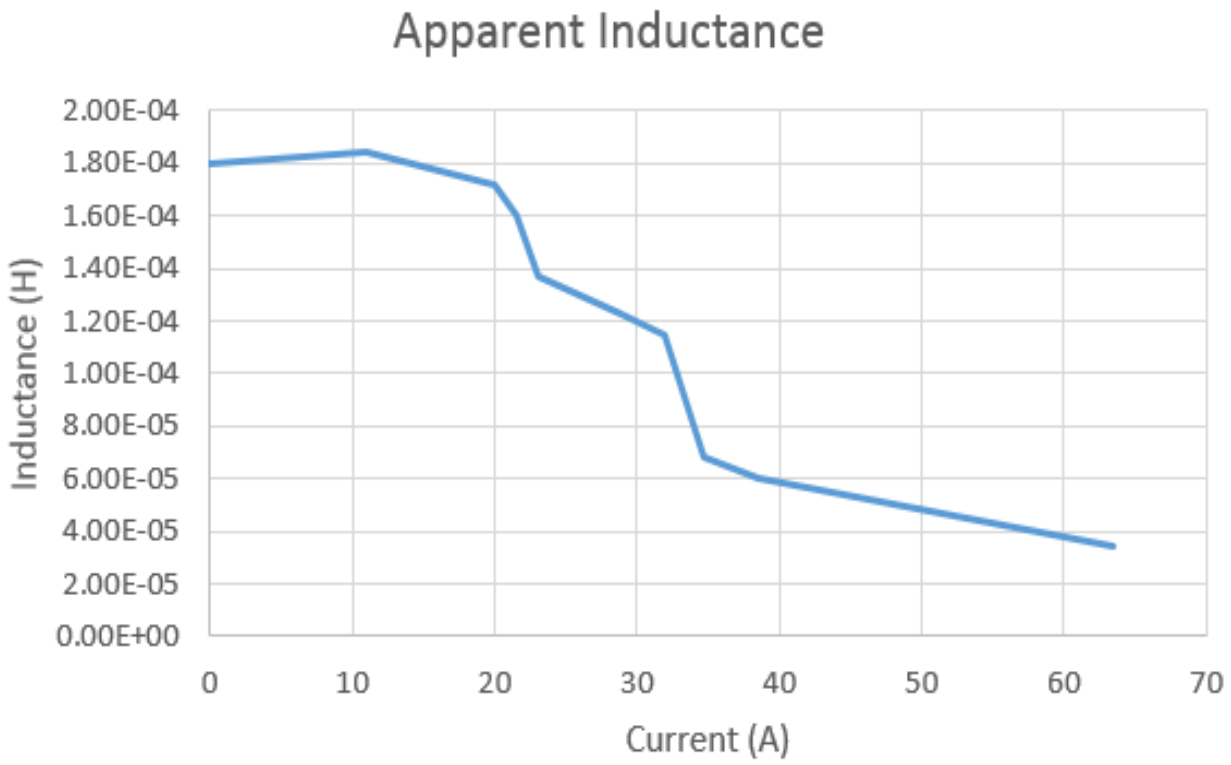

Figure 31. L-apparent

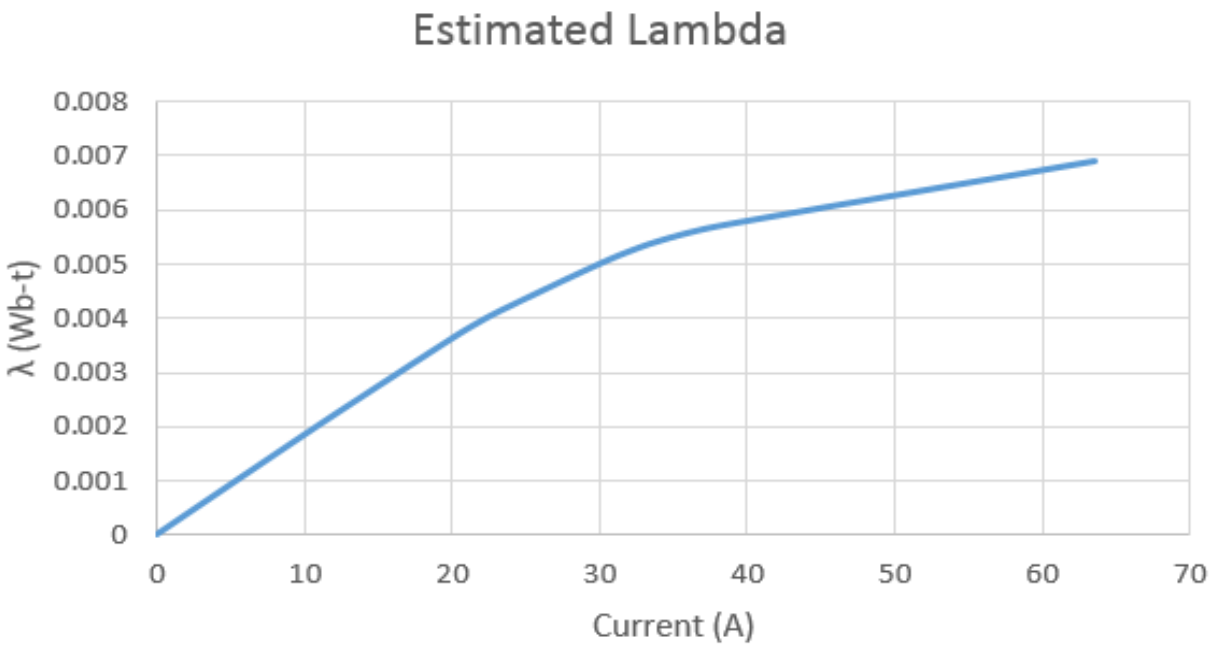

Figure 32. Estimated lambda

b. Three-Phase Inductor

Following the same procedure as for the single-phase inductor, the pulse test was conducted on a three-phase inductor, as seen in Figure 33, in the two configuration methods.

Figure 33. Three-phase inductor

i. **Common Mode Configuration**

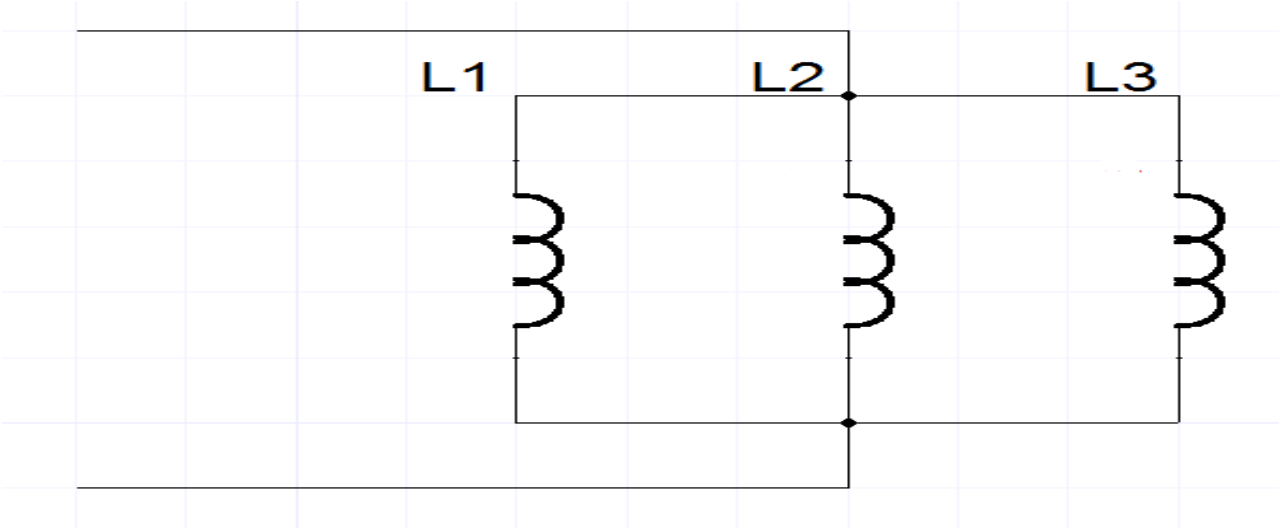

Figure 34. Common mode configuration

ii. **Differential Mode Configuration**

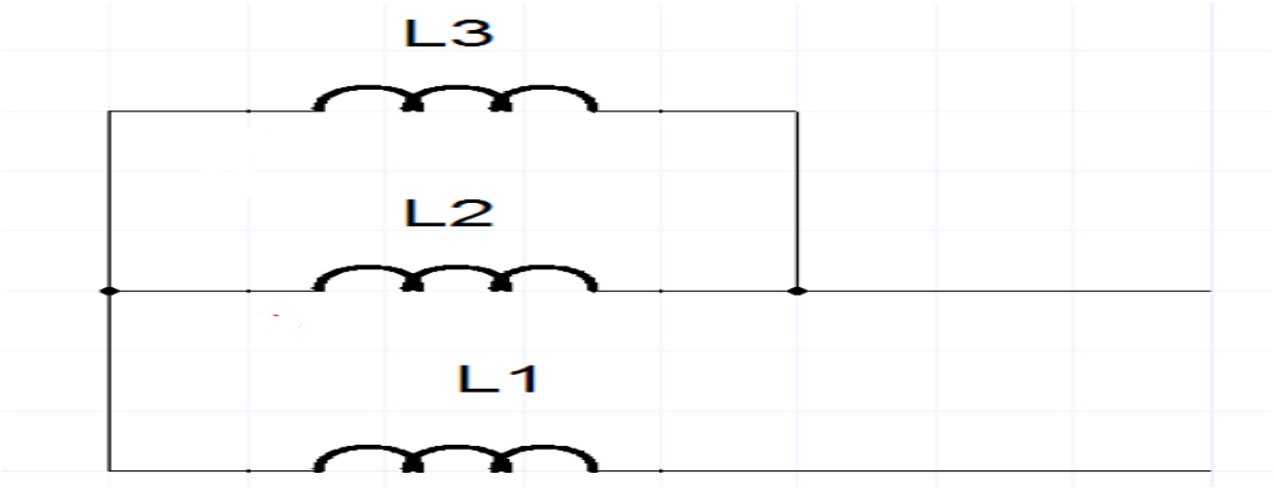

Figure 35. Differential mode configuration

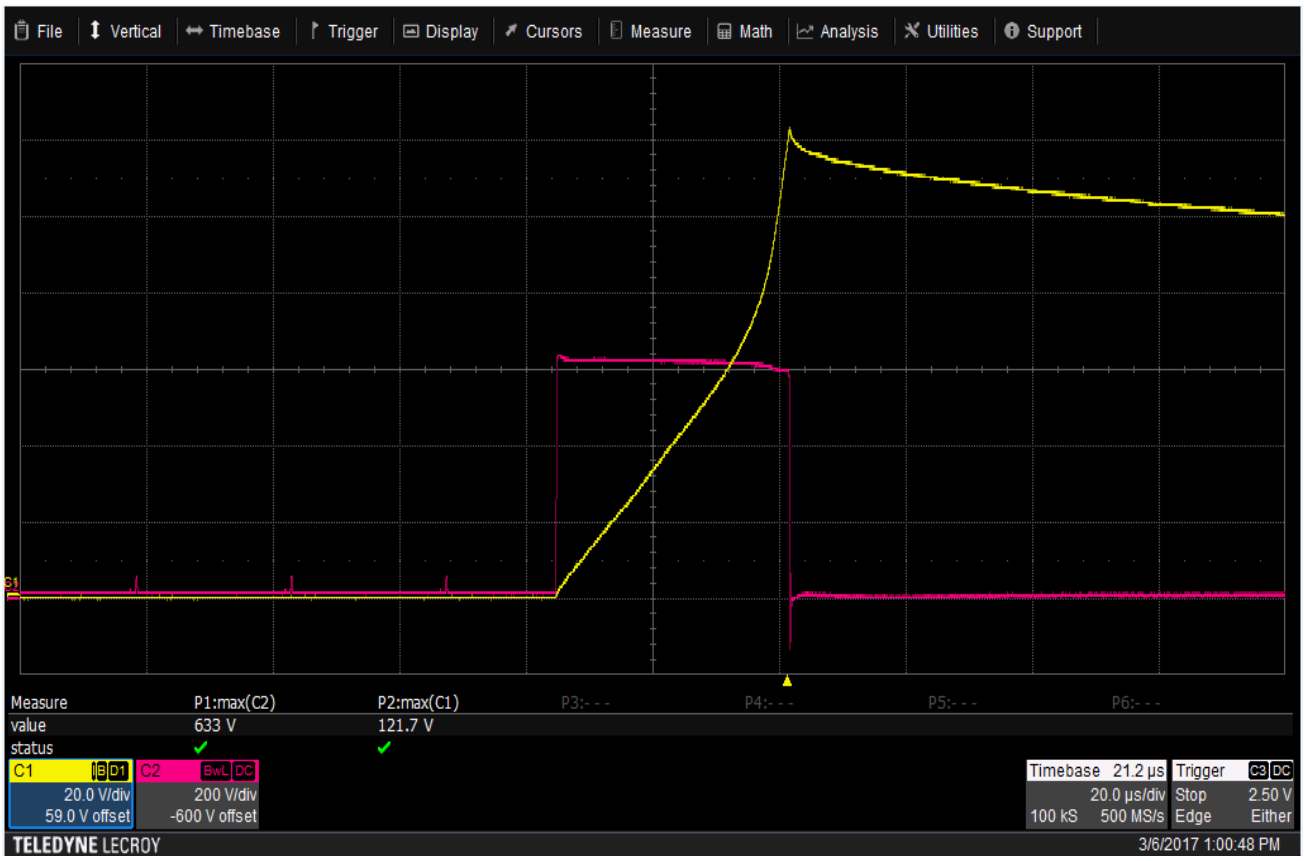

Figure 36. Saturation characteristic for DM

In the second measurement set-up, a single pulse test was performed on a 17.5Amps, 200uH inductor connected across the upper phase on the output of the drive. The data and results are presented below.

I_1	I_2	I_{ave}	ΔI	Δt	V_{ave}	λ	L
		0				0	2.00E-04
-6.40E-01	17.8	8.58	1.84E+01	8.40E-06	633	0.00252403	2.88E-04
1.78E+01	36.2	27	1.84E+01	8.60E-06	633	0.0079046	2.96E-04
4.22E+01	49.1	45.65	6.90E+00	3.00E-06	633	0.01322989	2.75E-04
5.09E+01	62.6	56.75	1.17E+01	4.20E-06	633	0.01496017	2.27E-04
64.2	83.5	73.85	1.93E+01	4.40E-06	633	0.01813685	1.44E-04
80.2	113	96.6	3.28E+01	3.20E-06	633	0.02048087	6.18E-05
99.4	123.8	111.6	2.44E+01	2.00E-06	633	0.02133318	5.19E-05

Table 3. Saturation characteristic results for DM configuration

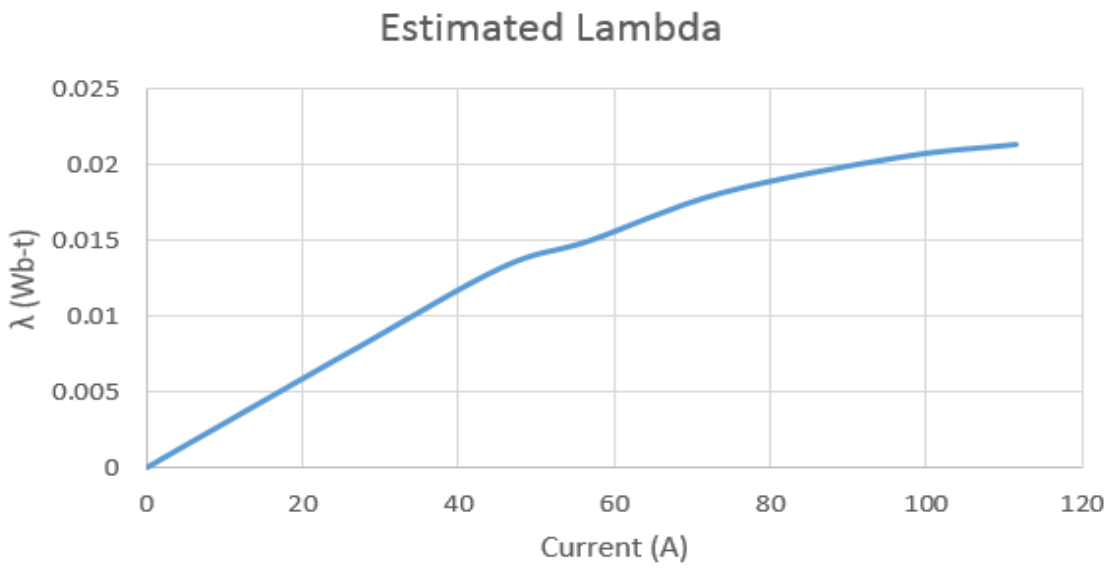

Figure 37. Estimated lambda for DM configuration

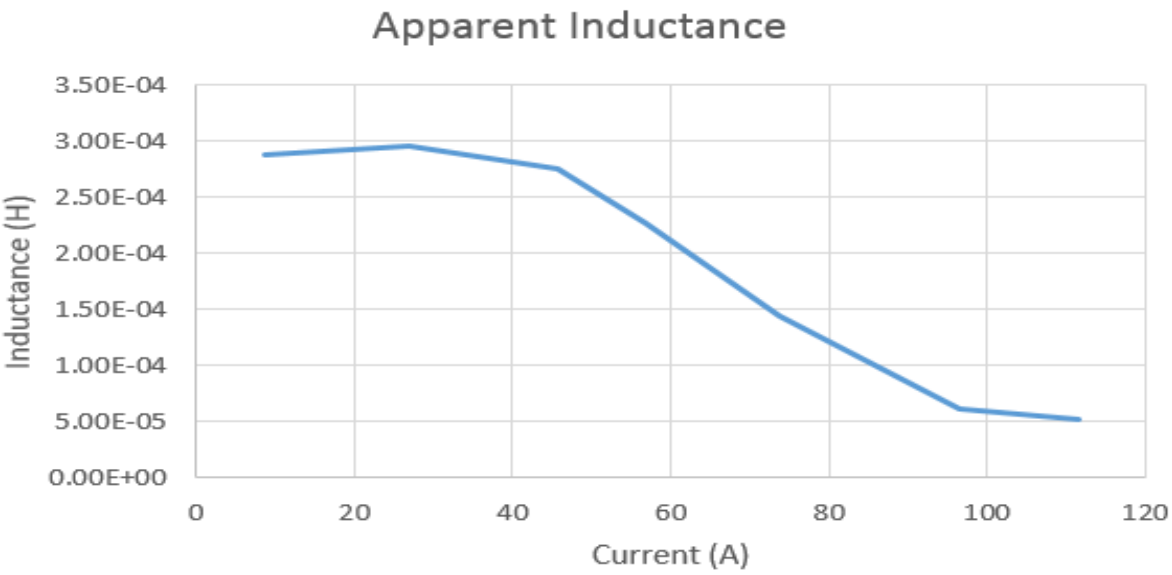

Figure 38. L-apparent for DM configuration

c. Common Mode Inductor

In the last measurement set-up, a single pulse test was performed on a common mode inductor, as seen in Figure 39, connected across the upper phase on the output of the drive. The data and results are presented below.

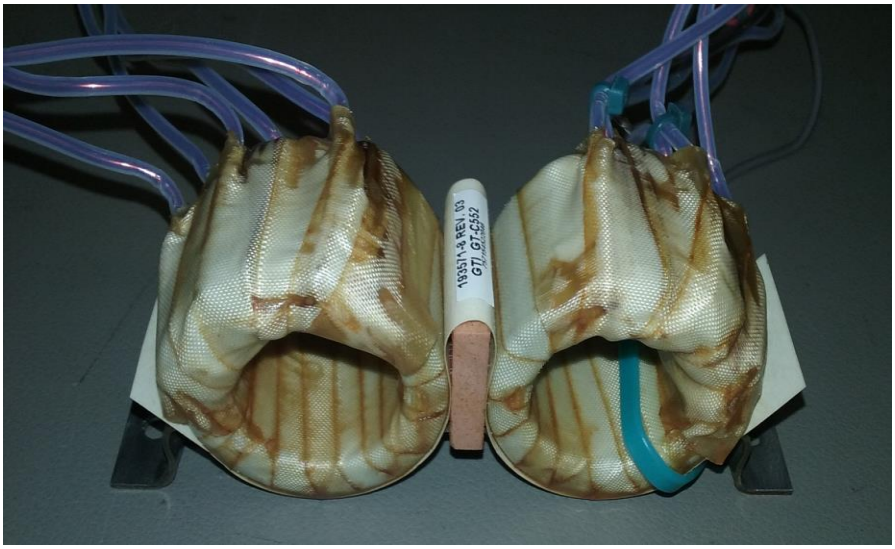

Figure 39. Common mode inductor

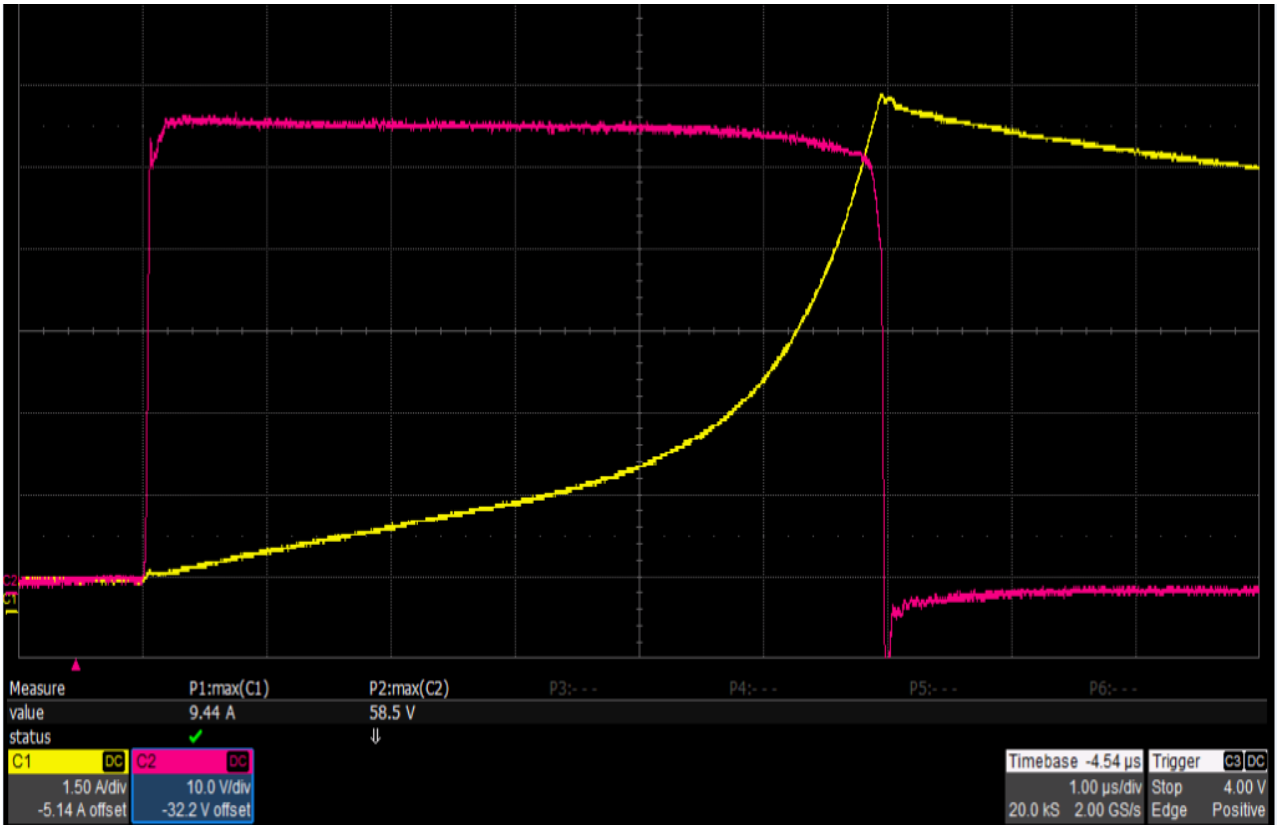

Figure 40. Saturation characteristic for CM inductor

I1	I2	Iave	ΔI	Δt	Vave	Λ	L
5.04E-01	9.00E-01	0.702	0.396	5.80E-07	58.5	26.325	8.568E-05
8.64E-01	1.09	0.977	0.226	3.90E-07	58.5	37.44	1.010E-04
1.12	1.33	1.225	0.21	5.10E-07	58.5	51.48	1.421E-04
1.56	1.81	1.685	0.25	6.00E-07	58.5	79.56	1.404E-04
1.8	2.02	1.91	0.22	4.20E-07	58.5	91.845	1.117E-04
1.96	2.35	2.155	0.39	6.00E-07	58.5	111.15	9.000E-05
2.23	2.7	2.465	0.47	3.80E-07	58.5	131.625	4.730E-05
3.32	4.14	3.73	0.82	4.30E-07	58.5	215.865	3.068E-05
4.22	5.32	4.77	1.1	4.00E-07	58.5	284.895	2.127E-05
5.4	8.08	6.74	2.68	4.70E-07	58.5	446.355	1.026E-05
8.08	9.38	8.73	1.3	2.10E-07	58.5	522.405	9.450E-06

Table 4. Saturation characteristic results for CM inductor

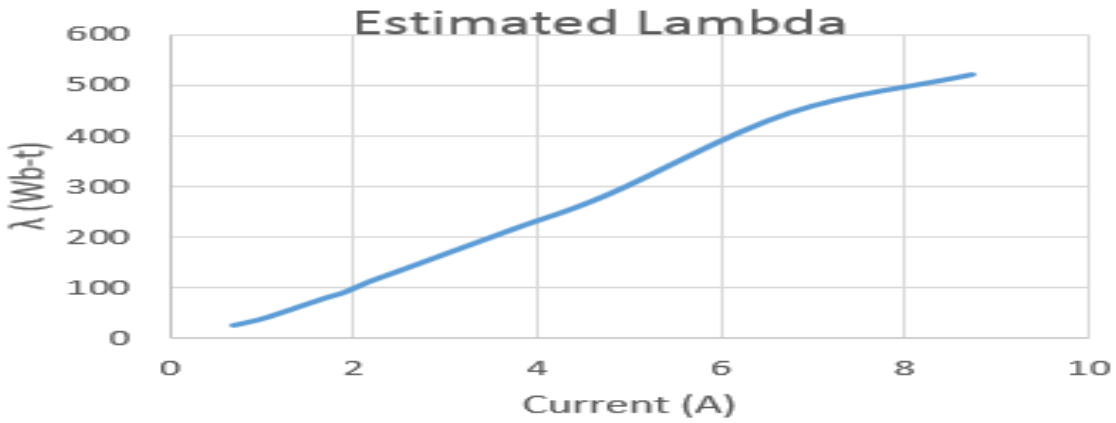

Figure 41. Estimated lambda for CM configuration

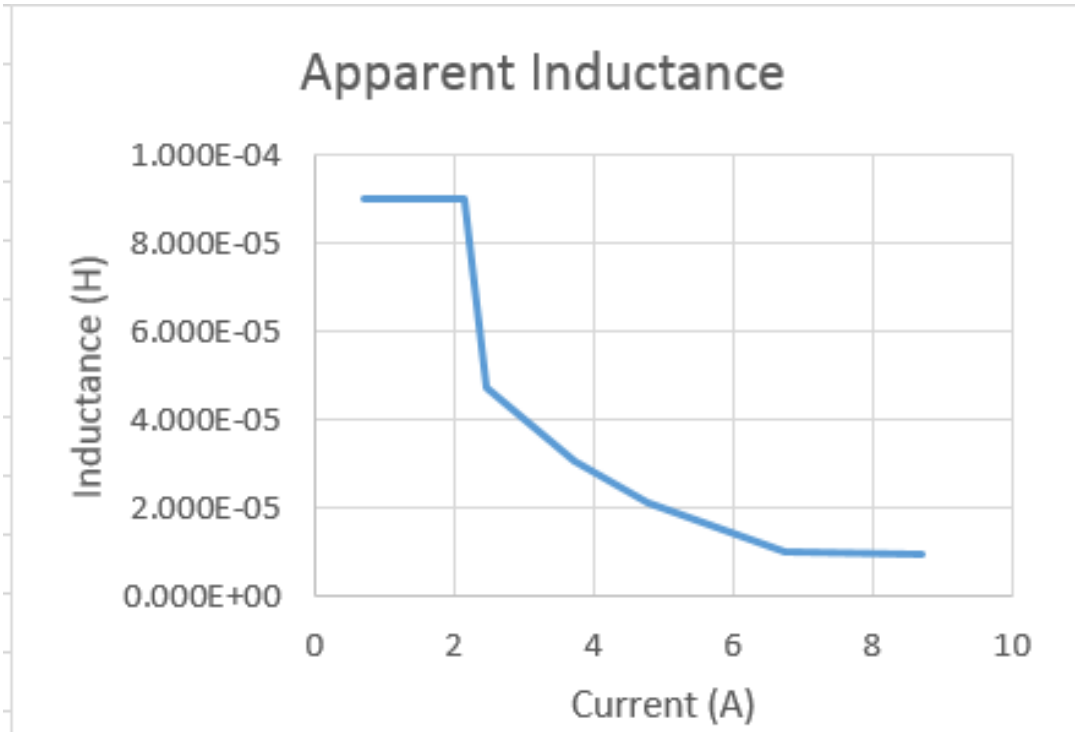

Figure 42. L-apparent for CM configuration

II. Frequency Versus Inductance Test

The purpose of this measurement is to model the inductor at a frequency which is high enough to include the self-resonant frequency. Even though PWM frequency is low, in order for the simulation to accurately predict the response of the dv/dt, the filter will need to be modeled in high frequency range which is excited by dv/dt.

a. Bias Test

In order the have an accurate model, the DC current bias test is an extremely important part of the data acquisition. When bias is applied, the inductance calculated at the operating point is not always equal to the inductance measured without bias, since the slope of the B-H curve varies. Therefore, it is important to test for the correct inductance at the maximum-rated DC current. Figure 43 shows the set-up required for the data acquisition.

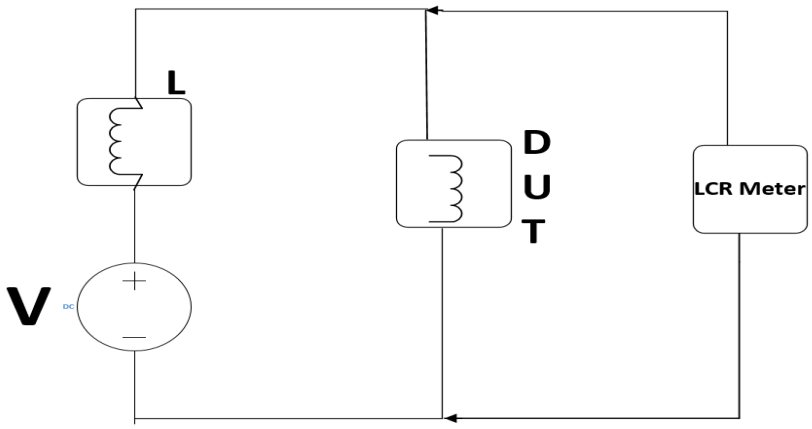

Figure 43. Frequency versus inductance test set-up

b. **Single-Phase Inductor Plus Bias**

Figure 44 shows the magnitude and the phase behavior of the single-phase inductor tested at different current bias levels.

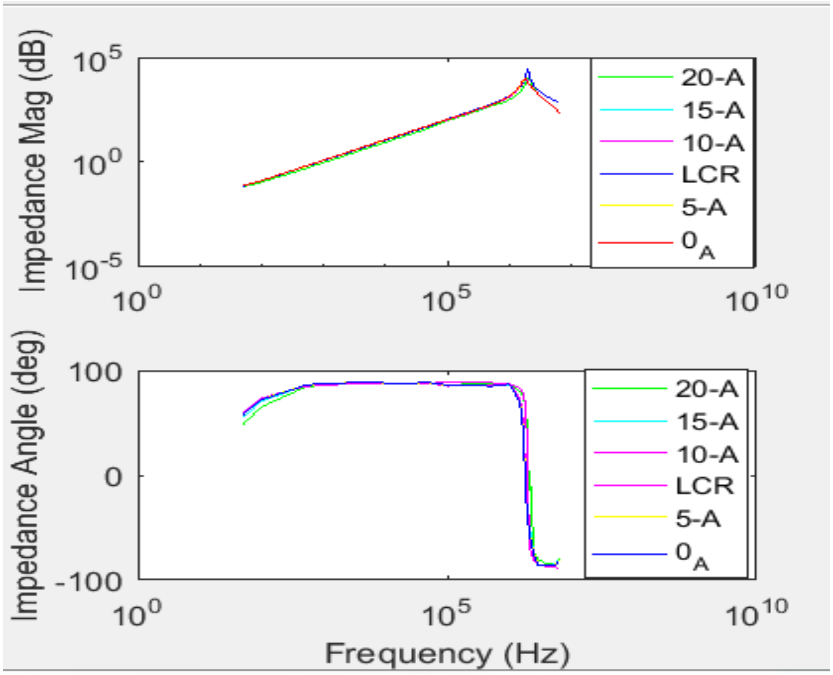

Figure 44. Magnitude and phase angle of the single-phase inductor with bias

c. Three-Phase Inductor Plus Bias

For this inductor, two configurations were taken into consideration: common mode and differential mode.

i. **Common Mode Configuration**

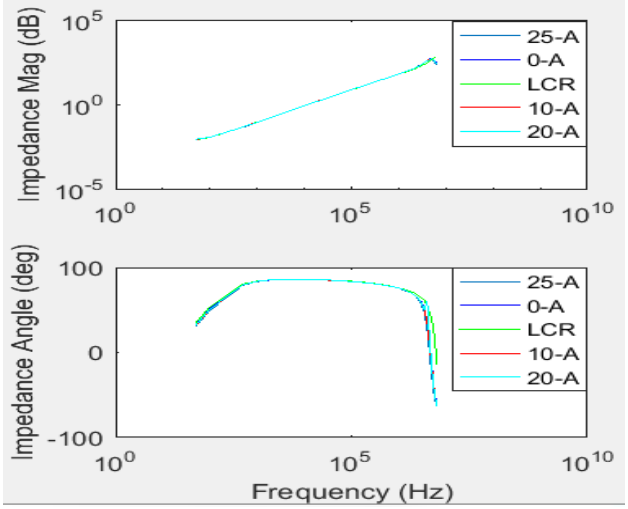

Figure 45. CM magnitude and phase angle of the three-phase inductor with bias

ii. Differential Mode Configuration

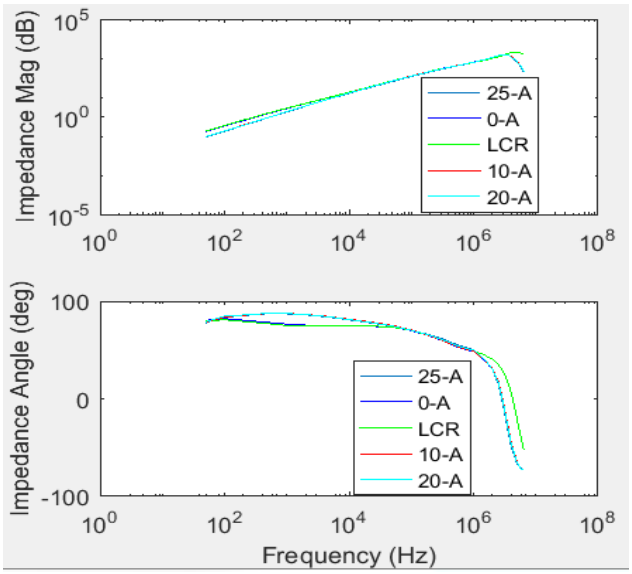

Figure 46. DM magnitude and phase angle of the three-phase inductor with bias

d. Common Mode Inductor Plus Bias

i. Common Mode Configuration

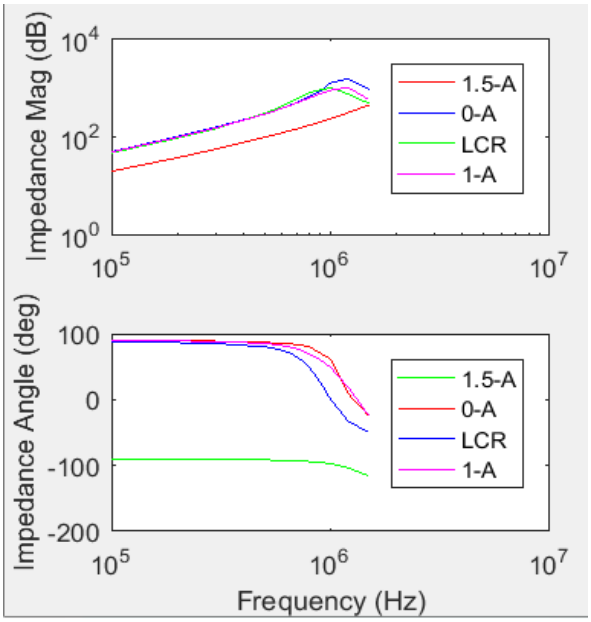

Figure 47. CM magnitude and phase angle of the CM inductor with bias

ii. Differential Mode Configuration

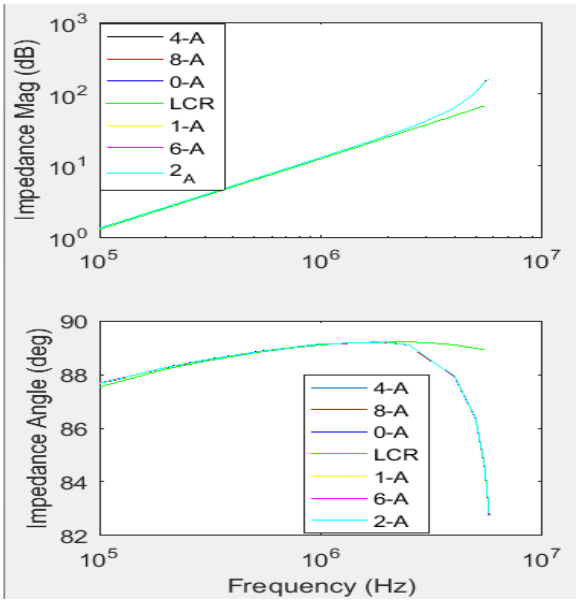

Figure 48. DM magnitude and phase angle of the CM inductor with bias

III. Circuit Modeling

In order to successfully model the inductors, a series of steps and software tools were utilized. A brief description of the steps taken are presented below.

a. GOSET

GOSET stands for Genetic Optimization System Engineering Tool. It is used in MATLAB for solving optimization problems. Primarily, it has been used to solve problems related to magnetics, electric machinery and power electronics. It has also been used to design inductors, brushless DC motors, power supplies and inverters and for the parameter identification of synchronous machines, induction machines and gas turbines [23]. For finding the best fit for the model, two types of files have been created. The .m files contain the parameters and formulas to generate the parameter values and plot the fitted curves. The .mat files were created to input the data obtained from the frequency vs. inductance measurement.

b. Single-Phase Inductor Filter Model

To obtain the parameter values for the circuit model, the data obtained from the frequency vs. impedance measurement, which represented the non-saturated values, was imported to GOSET. In order to obtain the saturated values of the inductor, the pulse test data was used in Simplorer to create a datasheet for the inductor.

For a single-phase inductor L_s and K can be ignored.

Generation Numb: 1000		
Gene No.	Description	Value
1	Rs	0.034324
2	Rp	29133.4179
3	Lp	0.00016352
4	Rw	3.5343
5	Cw	3.9045e-011

Table 5. Parameters value for single-phase inductor

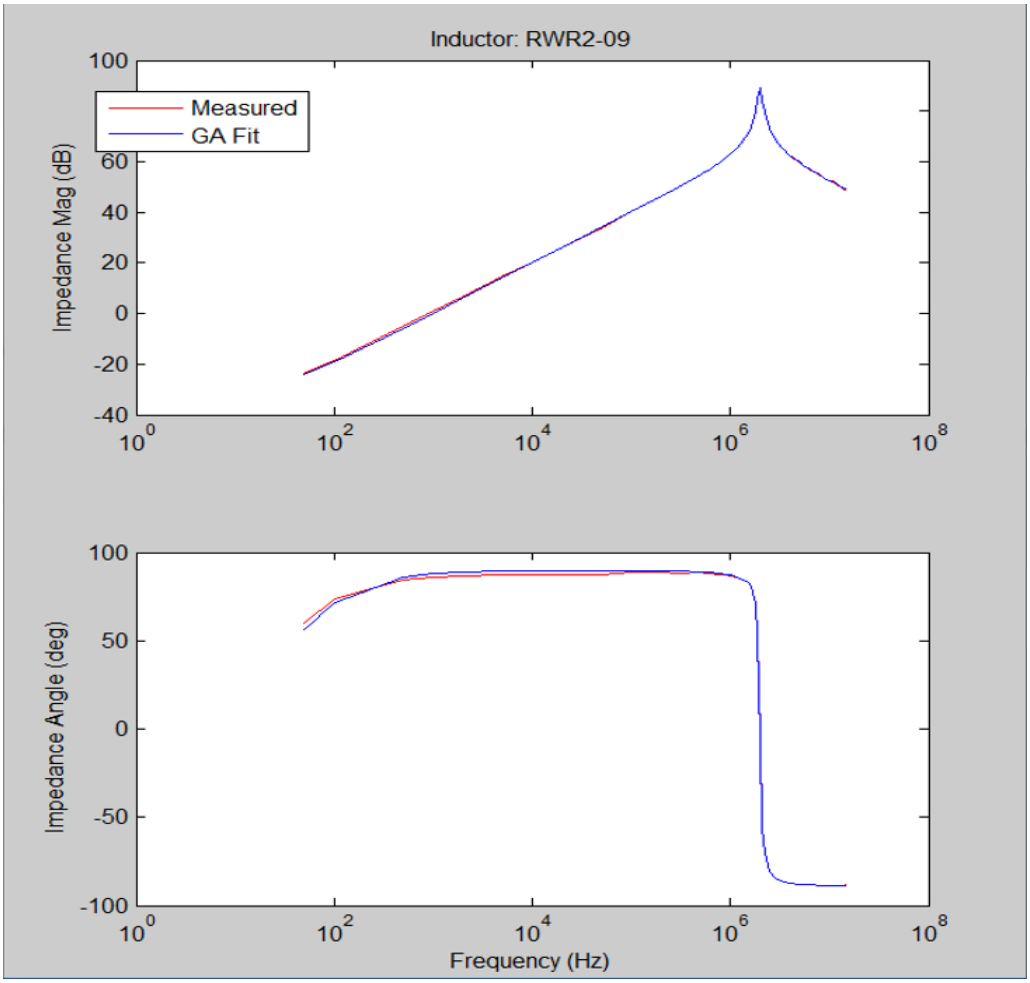

Figure 49. Single-phase inductor GOSET curve fit

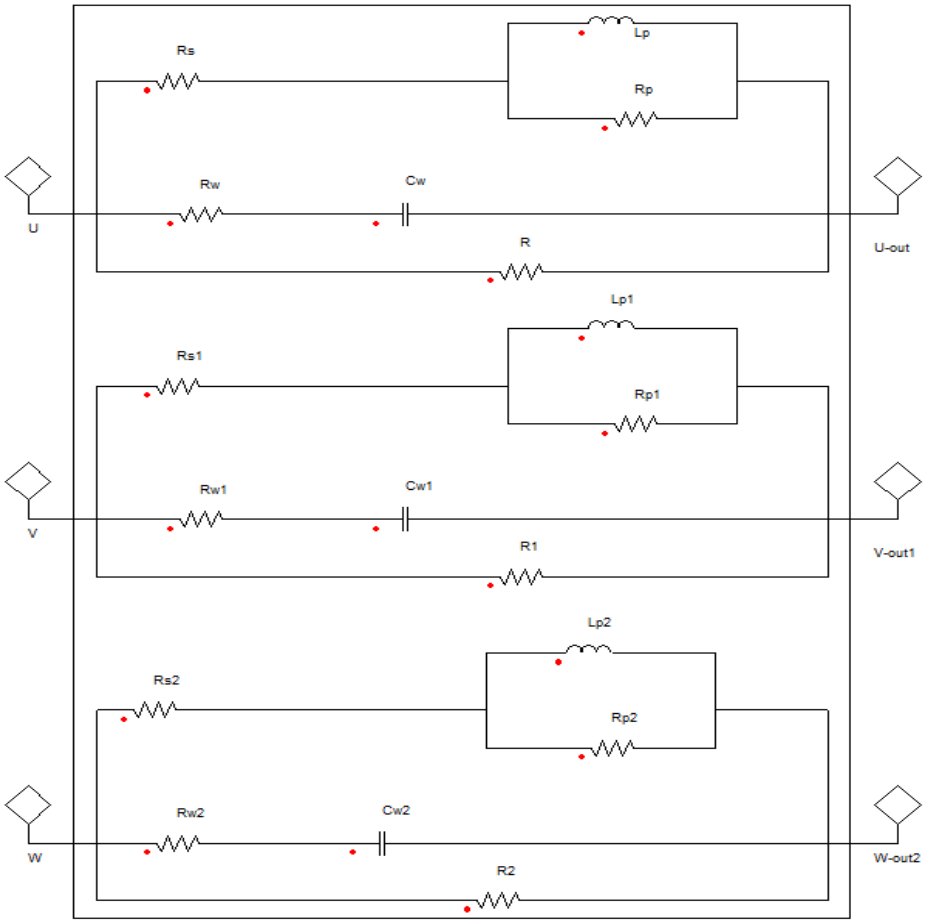

Figure 50. Circuit model for the single-phase inductor

c. Three-Phase Inductor Model

Below are the parameter values obtained from GOSET, the curve fit and the corresponding filter model.

Generation Numb:1000		
Gene No.	Description	Value
1	Rs	0.021776
2	Lp	0.00013324
3	Rp	297.1739
4	K	-0.43292
5	Rw	56.6505
6	Cw	4.195e-011
7	Ls	1.6919e-005

Table 6. Parameters value for three-phase inductor

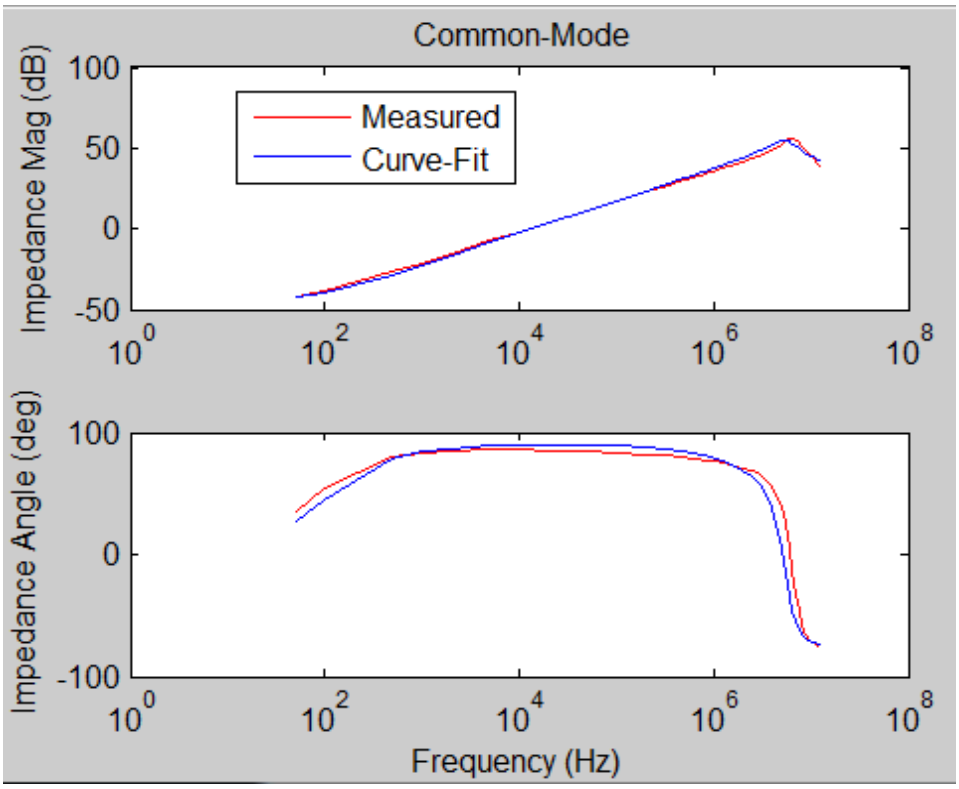

Figure 51. Three-phase inductor CM GOSET curve fit

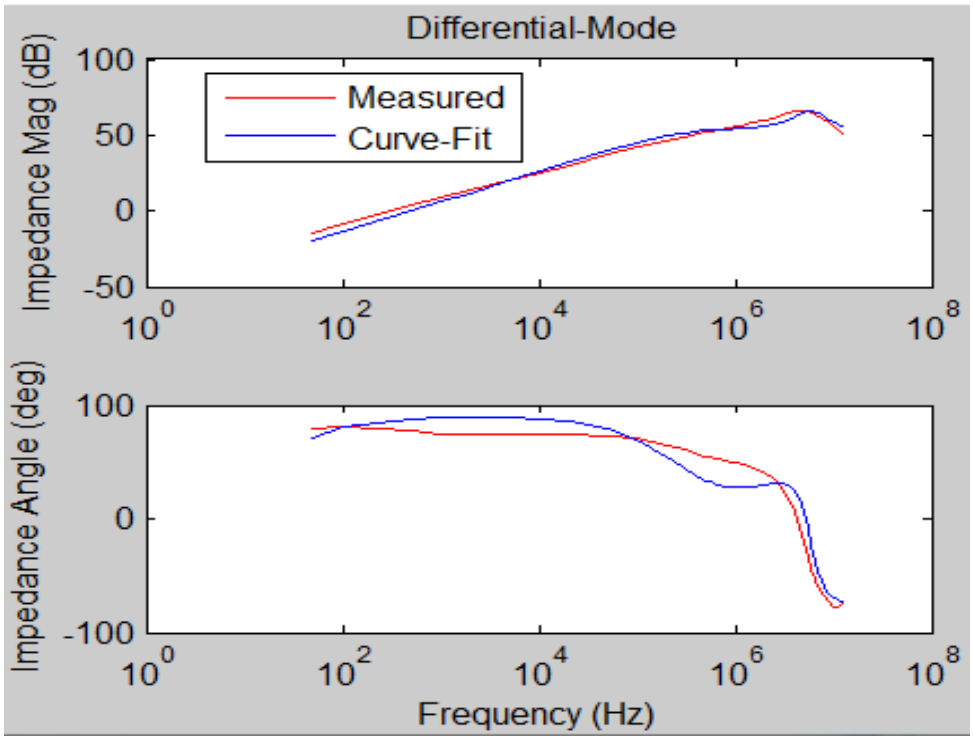

Figure 52. Three-phase inductor DM GOSET curve fit

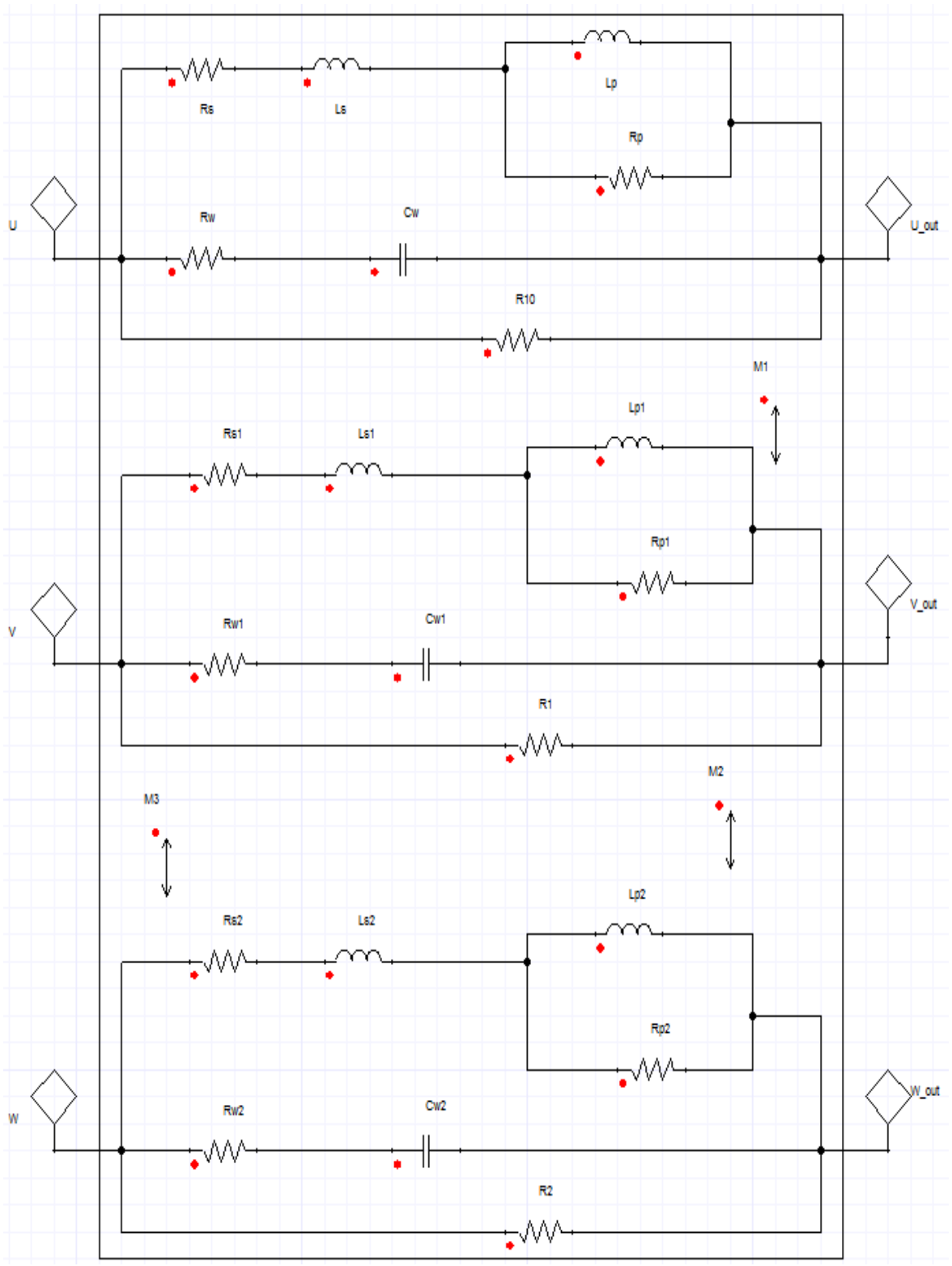

Figure 53. Three-phase inductor circuit model

d. Common Mode Inductor

In this model, due to the inductor winding the coupling, parameter K is equal to one for perfect coupling. Below are the parameter values obtained from GOSET, the curve fit and the corresponding filter model.

Gene values of the best individual

Generation Numb:1000

Gene No.	Description	Value
1	Rs	0.008646
2	Lp	7.4774e-005
3	Rp	988396.103
4	Rw	884.3451
5	Cw	7.3177e-011
6	Ls	1.3686e-006

Table 7. GOSET parameters for CM inductor

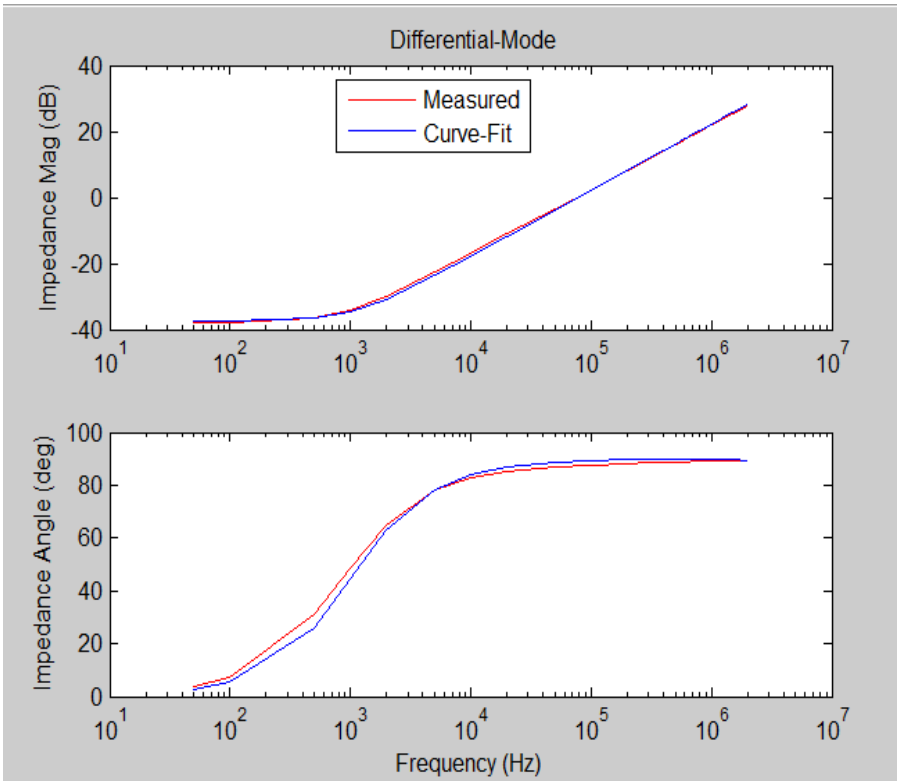

Figure 54. DM CM inductor GOSET curve fit

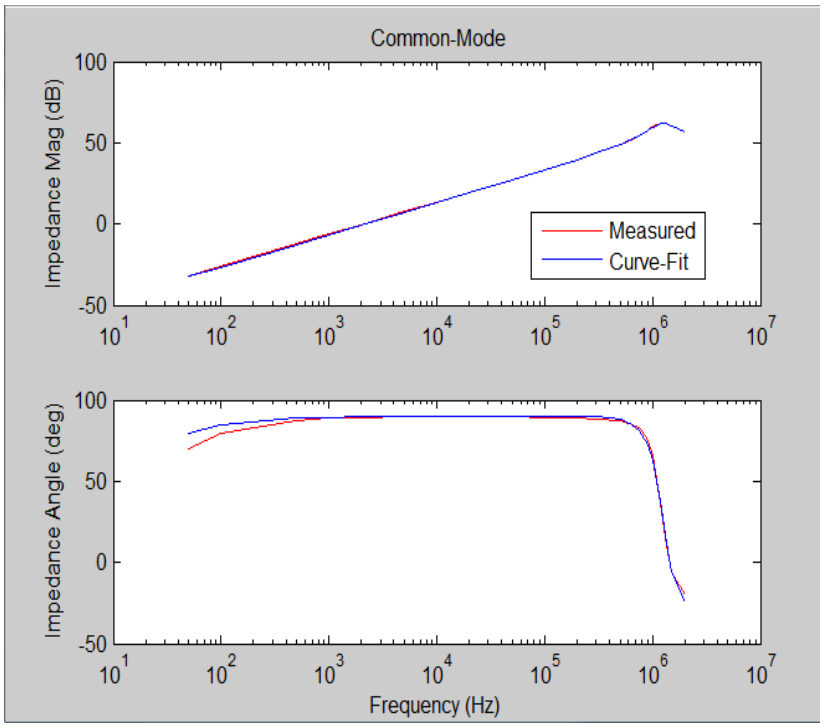

Figure 55. CM CM inductor GOSET curve fit

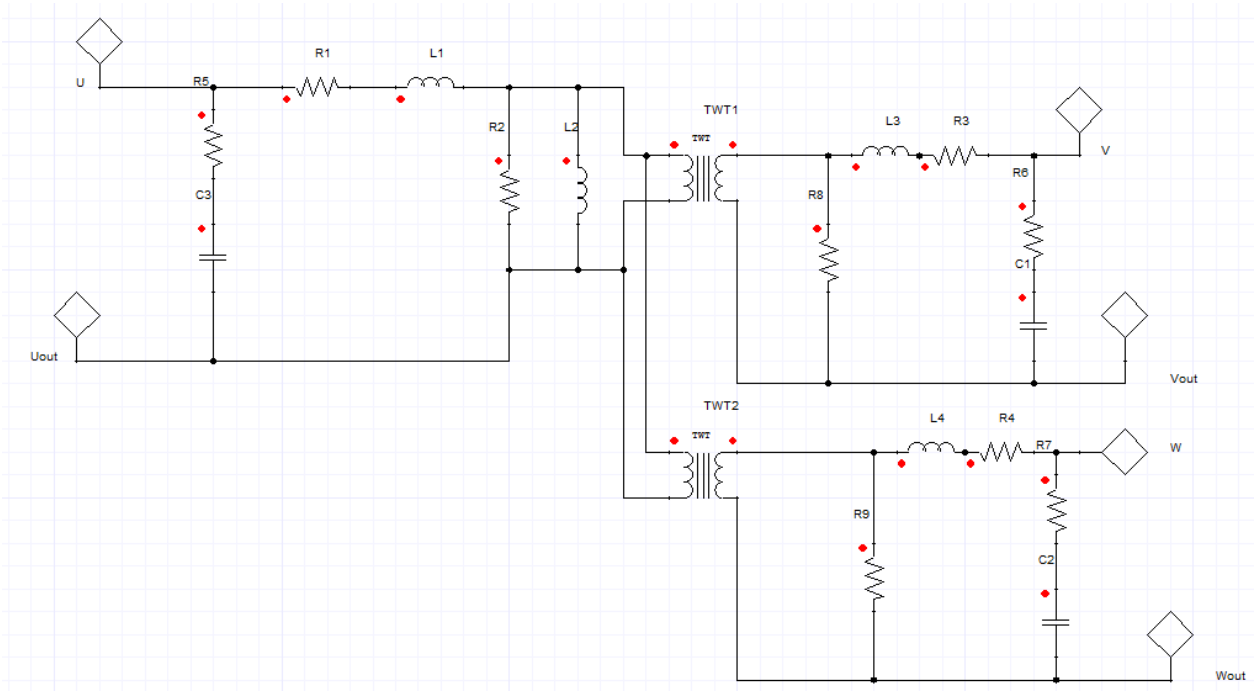

Figure 56. CMC circuit model

e. Model with Saturation

Because the CM inductor is saturated at a low current, the pulse test is a vital part of the modeling and has to be considered. For completeness, the model with saturation will also be considered for the single-phase inductor.

i. Single-Phase Inductor Model

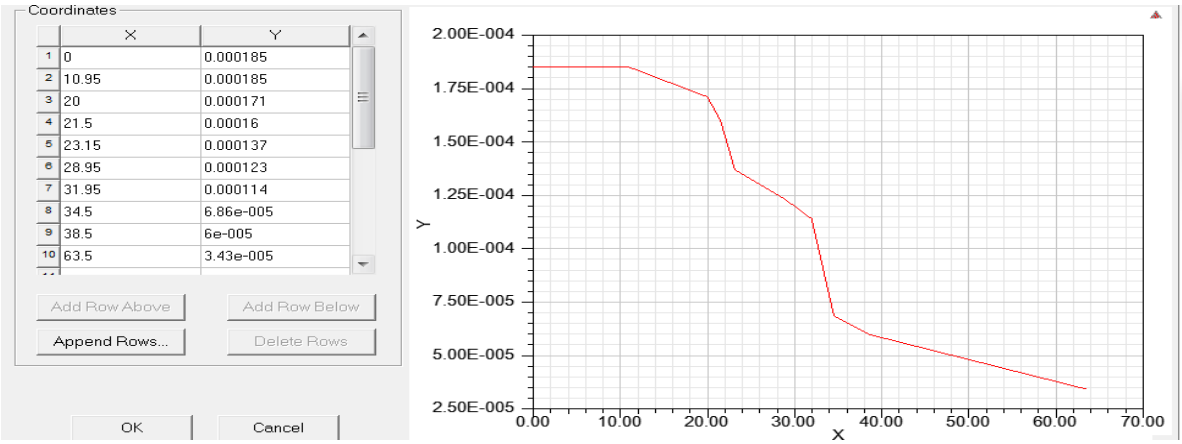

Figure 57. Simplorer saturated inductor model

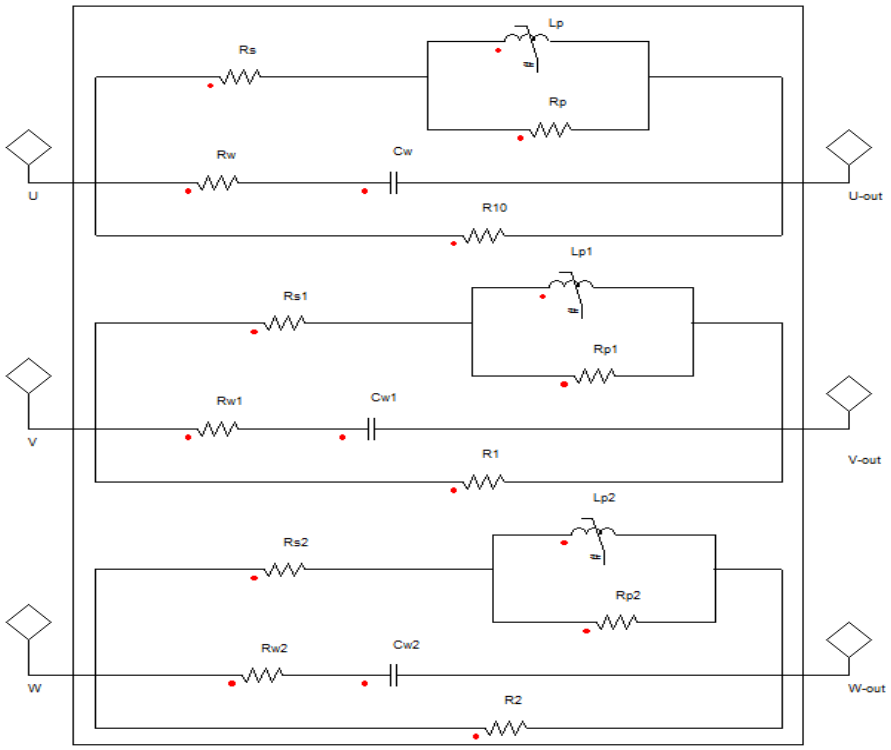

Figure 58. Circuit model with saturation

ii. Common Mode Inductor Model

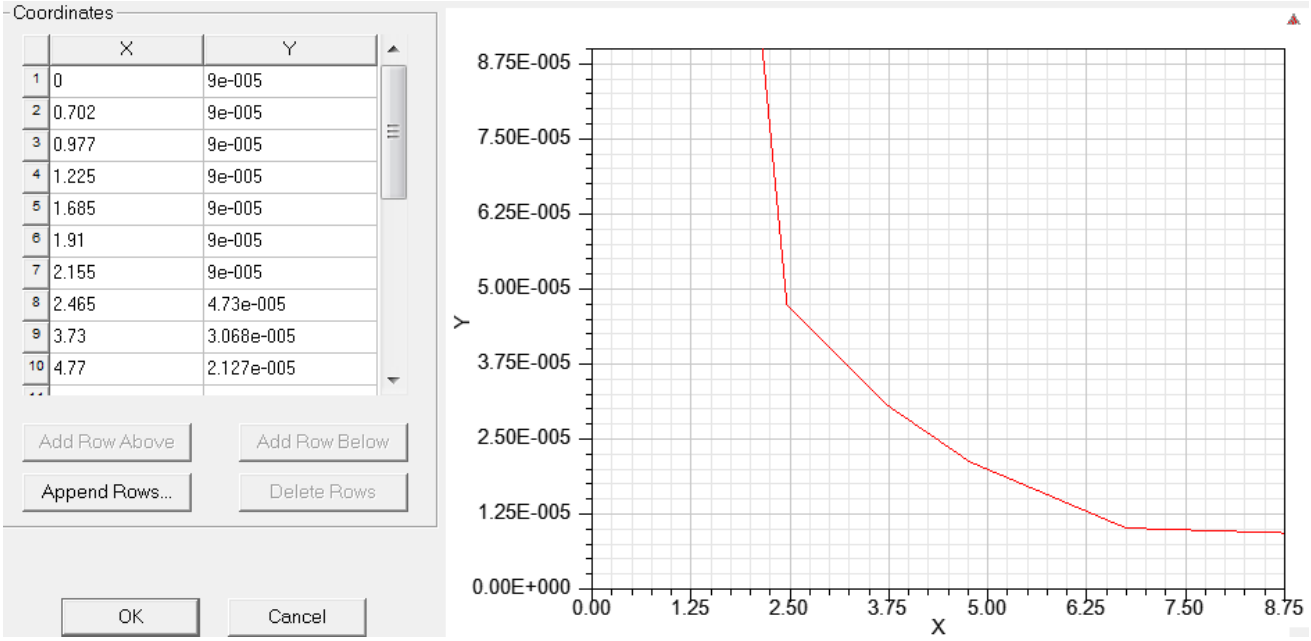

Figure 59. Simplorer saturated inductor curve

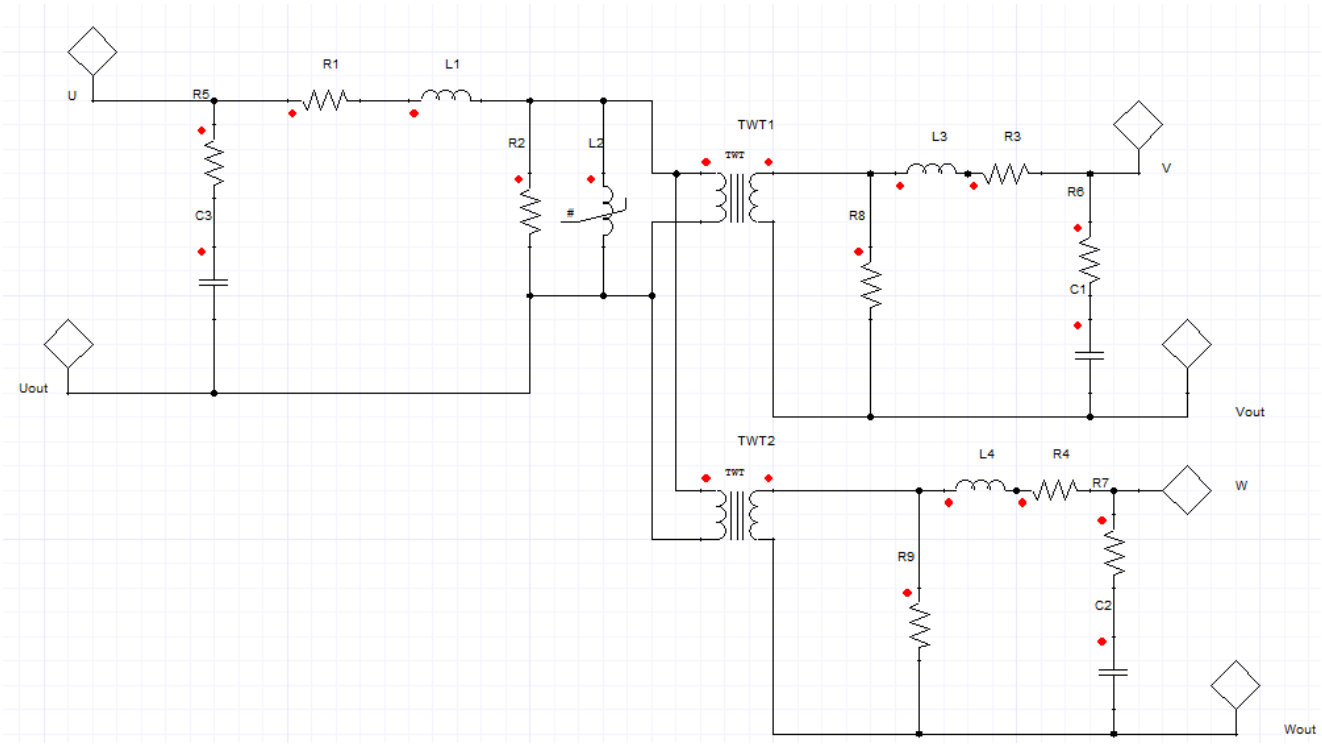

Figure 60. CM inductor circuit model with saturation

III. Simulation Consideration

In order to ensure that the new filter model performs as predicted and complies with the industry standards, the simulation was carried out both with and without the PE jumpers in the drive and at different frequency levels, including 5Hz, 45 Hz and 60 Hz. The simulation results were compared to the experimental results.

a. Jumpers Inserted or Removed

The PE jumpers terminal usually serve as a safety equipment ground with one jumper used for the AC line and one jumper for the DC bus of the drives. In ungrounded systems, metal (such as drive metal) can accrue electrical charge via leakage current. This results in voltages higher than the known safe touch potential of 50 V. Thus, all metallic parts of the drive, both internal and chassis, must be tied to the PE terminal.

The main issue for testing with PE jumpers both in and out is that drive systems can be connected to any distribution network. A standard distribution network can be classified into either a medium voltage delta or a low voltage wye, which can be further divided into solid grounded systems, floating systems and high resistance to ground (HRG) systems.

i. Solid Grounded System

In solid grounded systems, the drive is connected on the wye grounded side, thus sharing a common ground with the transformer. This shared ground becomes the PE of the drive. If a fault happens anywhere, it immediately returns to the transformer through the ground path, which then triggers the protection of the drive side. The advantage of this system is that the voltage is controlled. The line-to-line voltage and line-to-ground voltage is set by the transformer. The main disadvantage is that if a fault happens on the motor side, there will be a

large amount of current returning to the drive. The magnitude of this current can be very high and, as a result, there is a possibility for arch flash to occur. To prevent this, PE jumpers are added to help mitigate the effect of EMC and reduce the magnitude of the voltage to ground.

ii. Floating System

Floating systems have very similar configurations as grounded systems with the exception that the ground return path is removed. If a fault happens, there is no return path. As a result, these systems provide arch flash protection. The downside is that the magnitude of the voltage to ground is unknown due to the absence of ground return path. Since there are no true floating systems due to the presence of parasitic capacitances to the ground, one can say that the system is essentially parasitically grounded. This type of system acts as a parasitic boost converter. In a situation where a ground fault occurs, the voltage will increase and start to break down insulation. The peak of this voltage depends on the parasitic capacitance. In summary, in this type of system, the PE jumpers are removed and protection to ground is lost.

iii. High Resistance to Ground (HRG)

In high resistance to ground systems a resistor is added between the neutral and ground of the wye connected transformer. In this type of system, the voltage is controlled as it is in the solid grounded system, only with a greater magnitude. Usually, in this type of system the resistor is sized to support up to four times the leakage current. In the case of a ground fault, the current flowing in the resistor is small compared to the size of the resistor, which limits the amount of energy. Therefore, the arch flash problem is remediated. However, since the drive does not trip when the fault occurs (due to requiring a more complex mechanism to detect ground fault), it becomes almost impossible to localize a ground fault easily. In this type of system, the PE

jumpers are removed.

The purpose of simulating the model with both PE added and removed is primarily due to the fact that the users' distribution system is unknown. Therefore, it is important to test the model for all possible connections in order to ensure the accuracy of the performance of the system.

Chapter 4: Experimental and Simulation Results

4.1 Simulation Model

Figure 61 is the complete model of the VFD, including the filter, cable and the motor. This model is able to simulate line charging currents, common mode effects and reflected wave phenomenon. Drive rating is 480v, 60Hz, 22A. Motor 7.5Hp, 60Hz, 9.6A and 1170 RPM. Cable AWG 12 and 300ft.

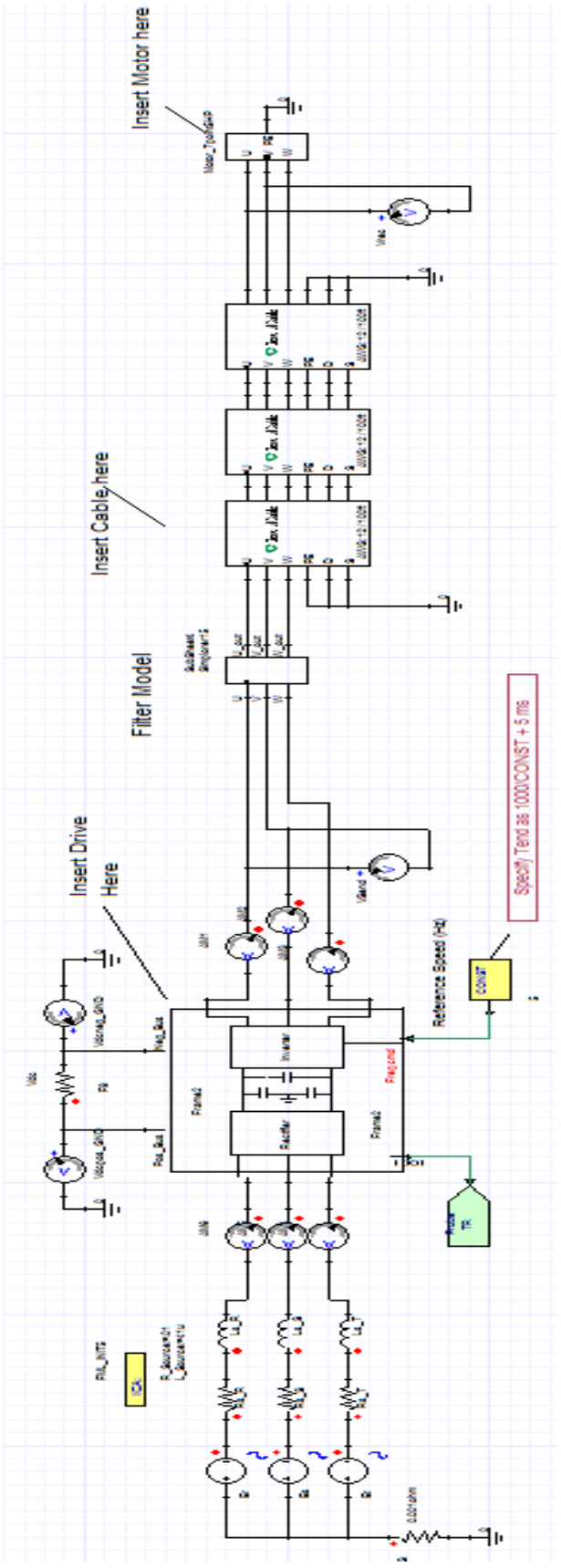

Figure 61. Complete model of VFD

4.2 Experimental Versus Simulation Results without Filter

I. Experimental Versus Simulation Results without Filter at 45Hz

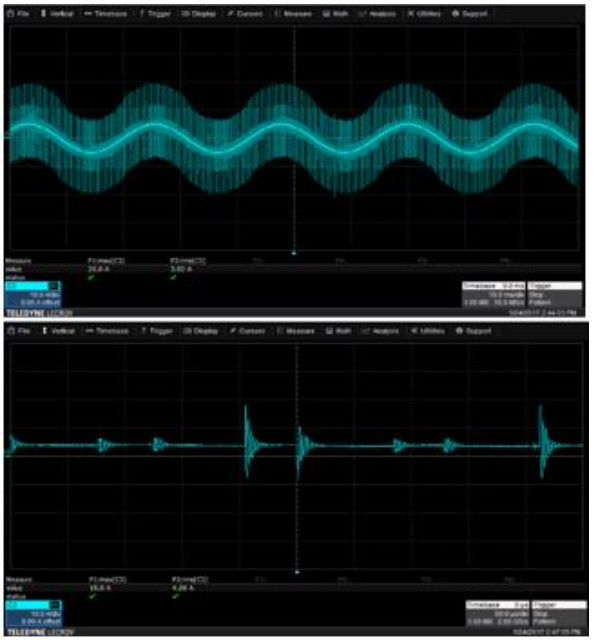

Figure 62. Phase current experiment

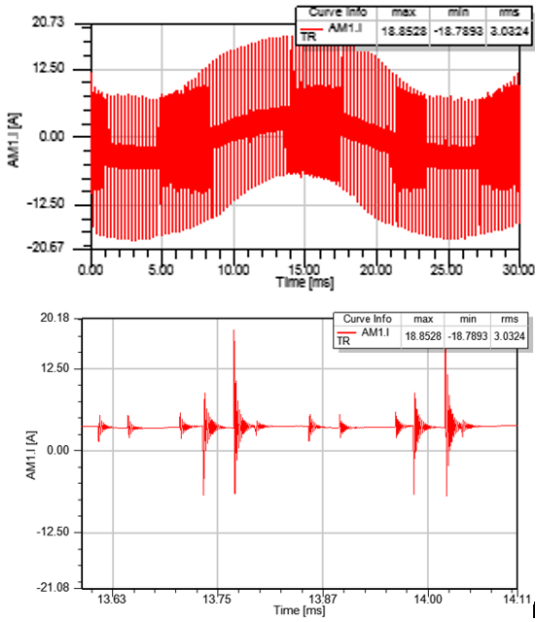

Figure 63. Phase current simulation

Figure 64. Send/rec voltage experiment

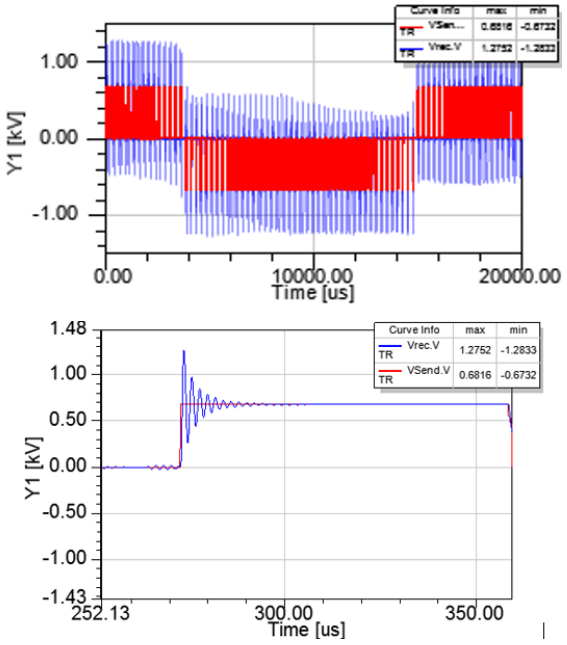

Figure 65. Send/rec voltage simulation

Figure 66. CM current experiment

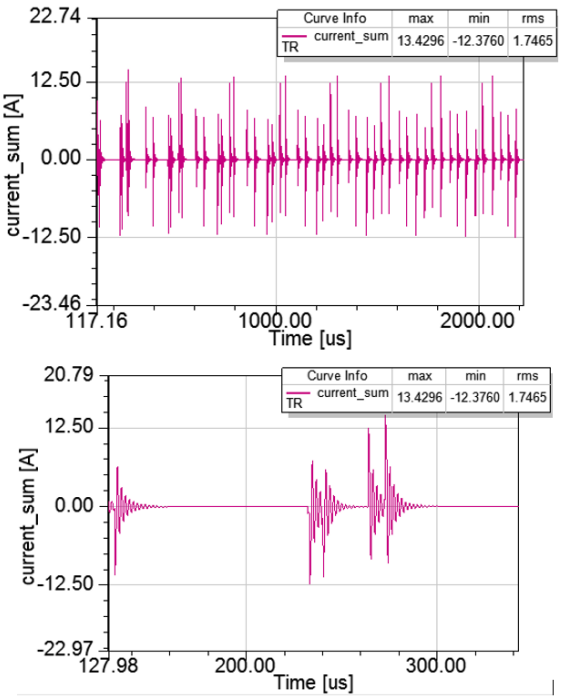

Figure 67. CM current simulation

II- Summary Tables

60 Hz			
Peak	Vsend/Vrec (V)	Phase current (A)	CM Current (A)
Experiment	700 / 1310.0	19.58	13.50
Simulation	681.6 / 1333.3	19.25	14.035
Jumpers removed			
Experiment	712/ 1280.0	18.71	2.57
Simulation	681.6 / 1287.9	17.89	1.14

Table 8. Data without filter at 60 Hz

45 HZ			
Peak	Vsend/Vrec (V)	Phase current (A)	CM Current (A)
Experiment	688 / 1270.0	18.57	13.71
Simulation	681.6 / 1275.2	15.1	13.43
Jumpers removed			
Experiment	712/ 1280	17.89	2.7
Simulation	681.6 / 1254.9	16.61	1.24

Table 9. Data without filter at 45 Hz

5 Hz			
Peak	Vsend/Vrec (V)	Phase current (A)	CM Current (A)
Experiment	700 / 1280	15.57	19.7
Simulation	682.2 / 1292.1	14.22	24.94
Jumpers removed			
Experiment	712/ 1310	14.0	3.1
Simulation	681.9 / 1282.6	11.92	2.35

Table 10. Data without filter at 5 Hz

4.3 Experimental and Simulation Results with Filter at 45Hz

I- Single-Phase Inductor

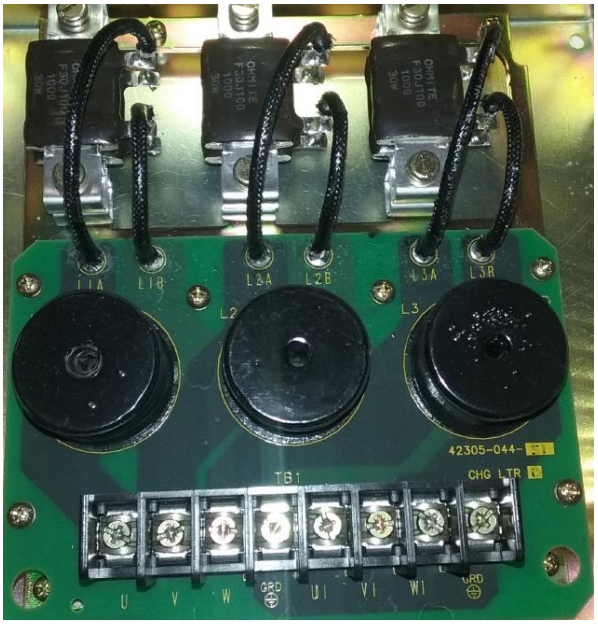

Figure 68. Experimental filter

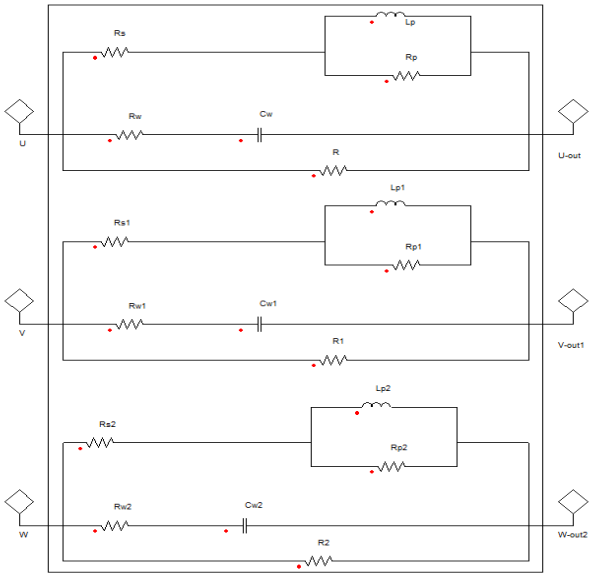

Figure 69. Simulation filter

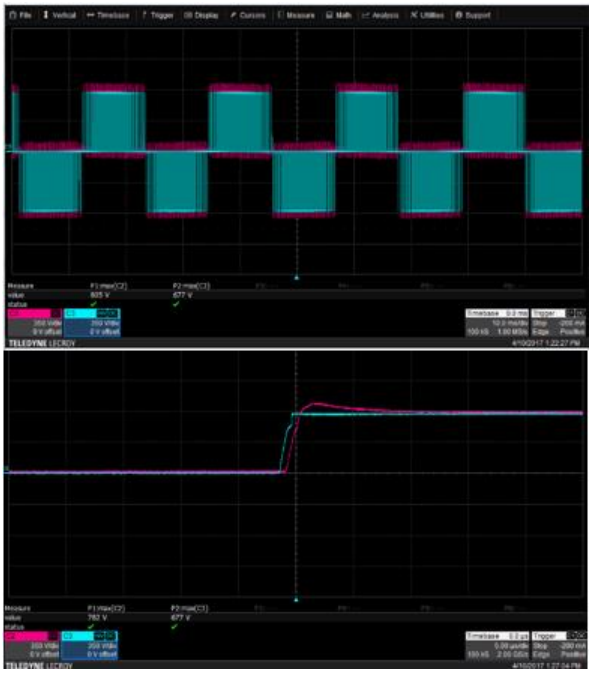

Figure 70. Voltage send/rec experiment

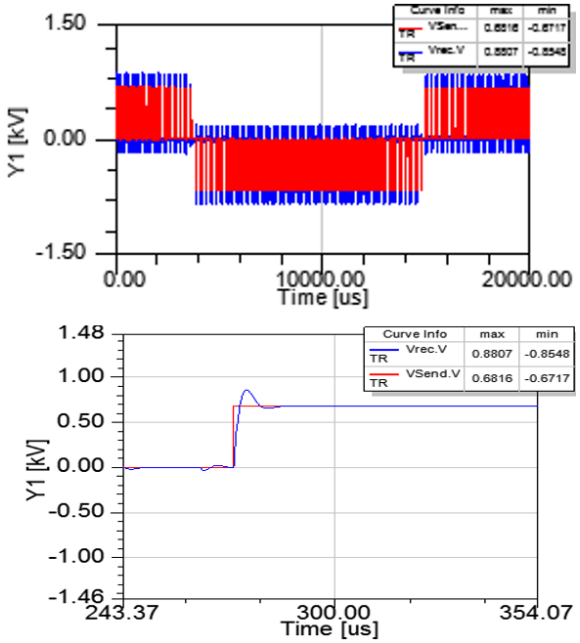

Figure 71. Voltage send/rec simulation

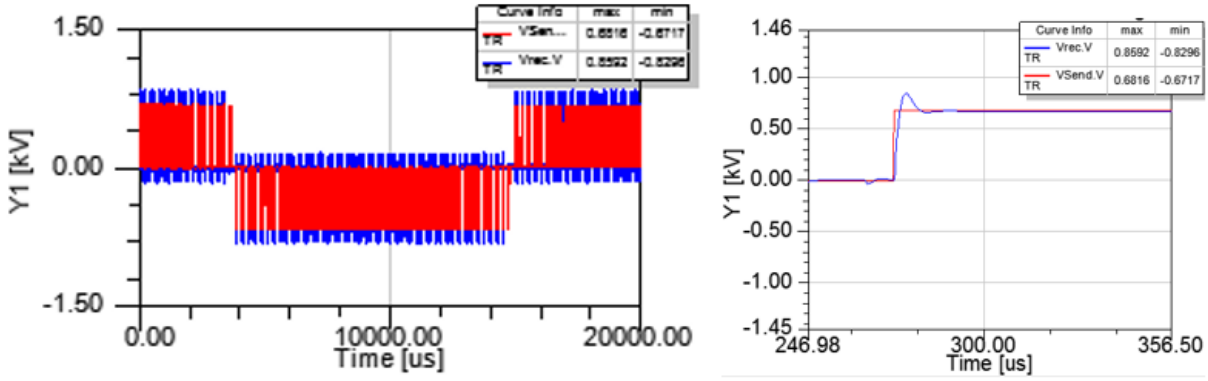

Figure 72. Send/rec motor end voltage with saturation

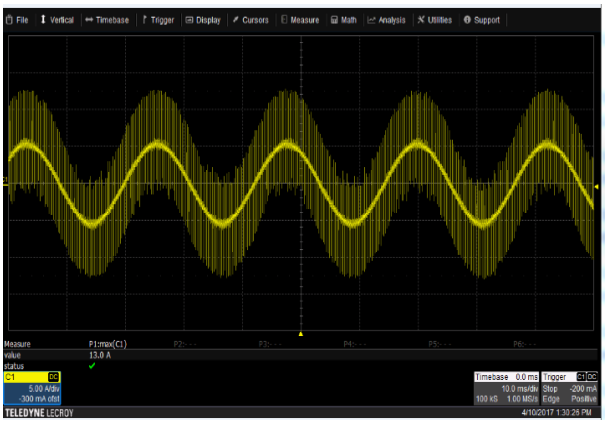

Figure 73. Phase current experiment

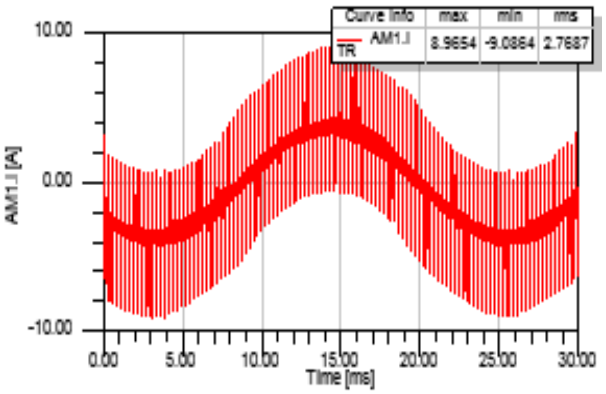

Figure 74. Phase current simulation

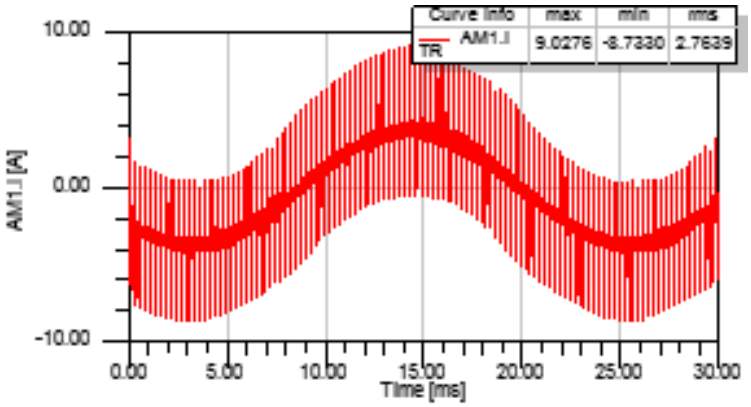

Figure 75. Motor phase current with saturation

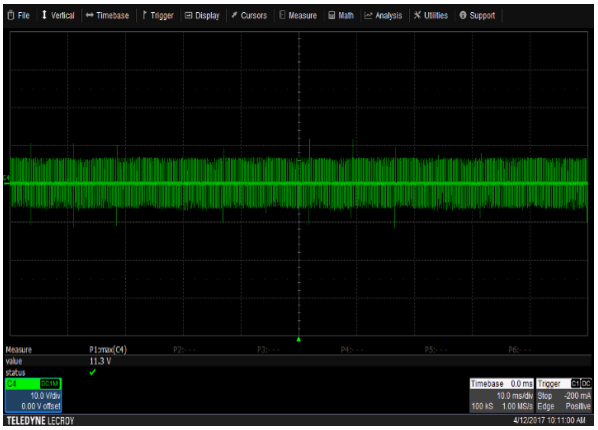

Figure 76. CM current experiment

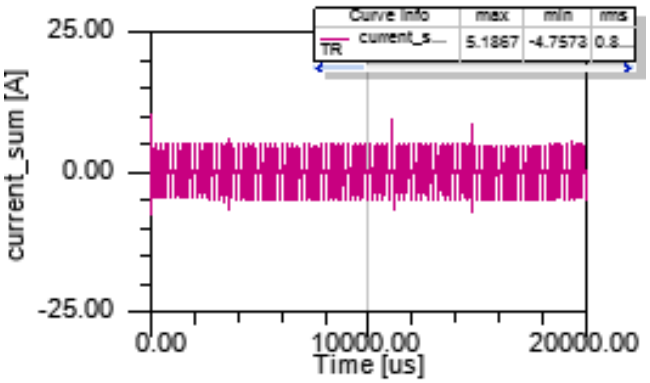

Figure 77. CM current simulation

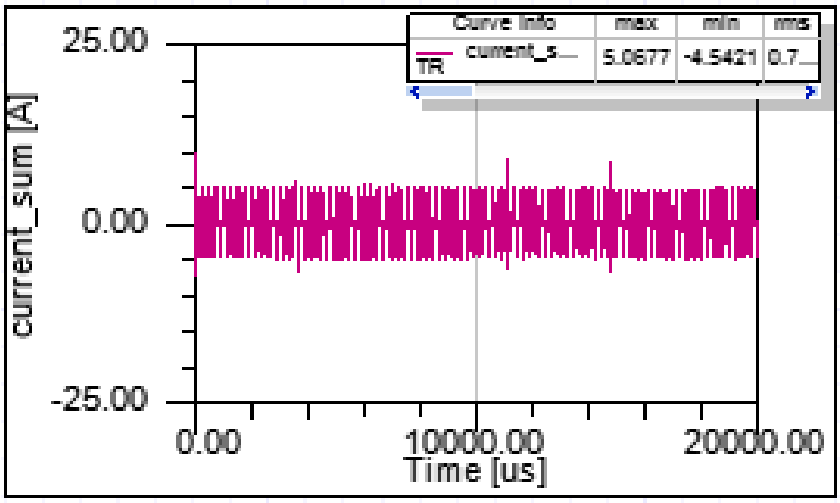

Figure 78. Common mode current with simulation

II. Summary Tables

60 Hz			
	Vsend /Vrec (V)	Motor Phase Current peak (A)	CM Current(A)
Experiment	677 / 805	12.8	6.4
Simulation	681.6 / 882.0	9.94	5.17
W/Saturation	681.6 / 860.3	10.05	5.19

Table 11. Filter with single-phase inductor at 60Hz

45 Hz			
	Vsend /Vrec (V)	Motor Phase Current peak (A)	CM Current(A)
Experiment	677 / 805	13.0	6.3
Simulation	681.6 / 880.7	8.97	5.19
W/Saturation	681.6 / 859.6	9.03	5.07

Table 12. Filter with single-phase inductor at 45Hz

5 Hz			
Peak	Vsend /Vrec (V)	Motor Phase Current peak (A)	CM Current(A)
Experiment	688 / 828	14.3	12.7
Simulation	681.6 / 882.6	4.84	10.02
W/Saturation	681.6 / 865.5	4.74	9.79

Table 13. Filter with single-phase inductor at 5Hz

60 Hz			
	Vsend/Vrec (V)	Motor Phase Current peak (A)	CM Current (A)
Experiment	677 / 782	11.0	2.0
Simulation	680.0 / 885.3	8.56	1.13
W/Saturation	680.0 / 841.8	8.56	1.12

Table 14. Filter with single-phase inductor with jumpers out at 60 Hz

45 Hz			
	Vsend/Vrec (V)	Motor Phase Current peak (A)	CM Current (A)
Experiment	665/ 782	11.0	2.70
Simulation	680.0 / 860.6	7.86	1.30
W/saturation	680.0 / 839.5	7.83	1.30

Table 15. Filter with single-phase inductor with jumpers out at 45 Hz

5 Hz			
	Vsend/Vrec (V)	Motor Phase Current peak (A)	CM Current (A)
Experiment	688 / 793	12.6	2.70
Simulation	688.1 / 869.3	4.24	2.36
W/Saturation	688.0 / 852.4	4.16	2.36

Table 16. Filter with single-phase inductor with jumpers out at 45 Hz

4.4 Experimental Versus Simulation Results with Filter at 45Hz

I. Three-Phase Inductor

Figure 79. Three-phase experimental filter

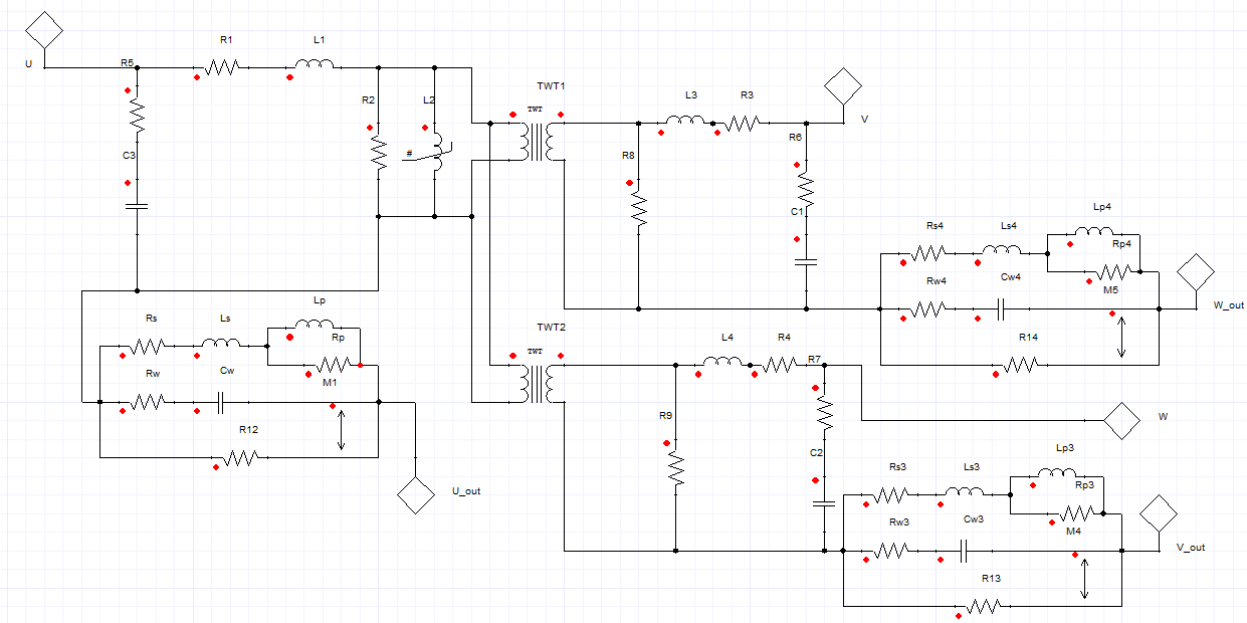

Figure 80. Three-phase simulation model

Figure 81. Three-Phase Vsend/rec experiment

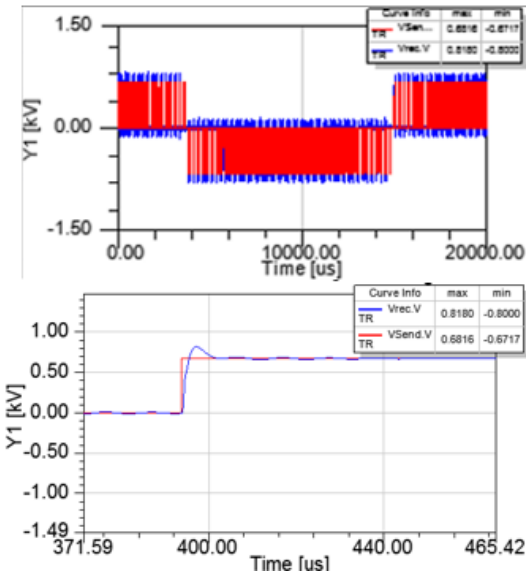

Figure 82. Three-phase V send/rec simulation

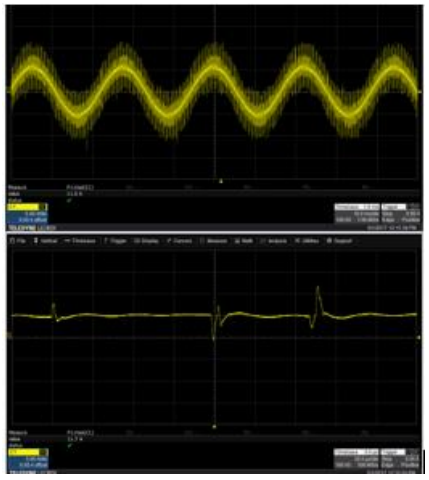

Figure 83. Phase current experiment

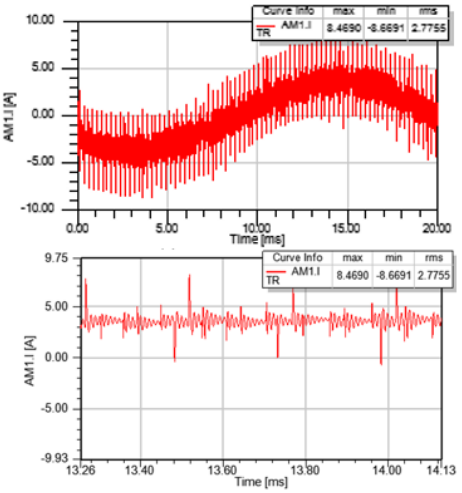

Figure 84. Phase current simulation

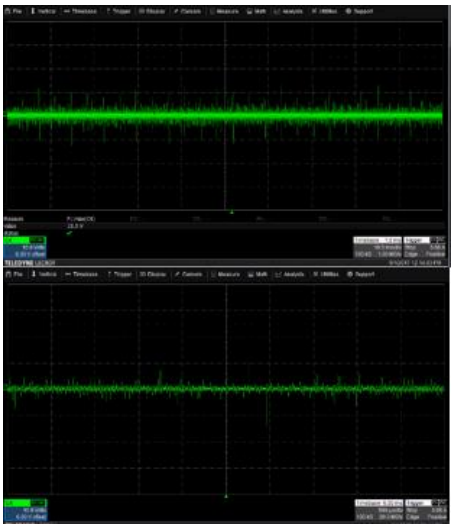

Figure 85. CM current experiment

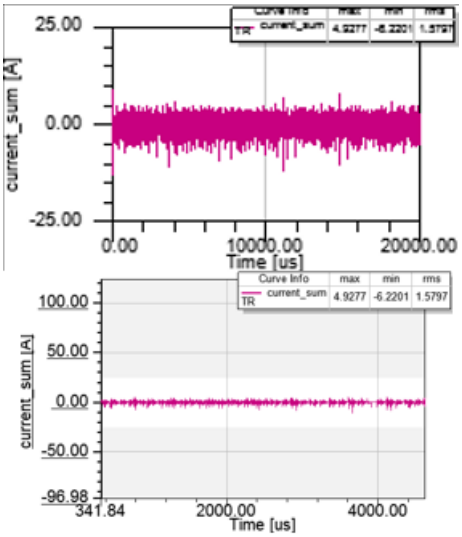

Figure 86. CM current simulation

II. Summary Tables

60 Hz			
	Vsend/Vrec (V)	Motor Phase Current peak (A)	CM Current (A)
Experiment	688 / 875	12.0	7.50
Simulation	681.6 / 812.9	9.53	5.96

Table 17. Filter with three-phase inductor at 60 Hz

45Hz			
	Vsend/Vrec (V)	Motor Phase Current peak (A)	CM Current (A)
Experiment	700 / 875.0	11.5	6.5
Simulation	681.6 / 818.0	8.47	4.93

Table 18. Filter with three-phase inductor at 45Hz

5Hz			
	Vsend/Vrec (V)	Motor Phase Current peak (A)	CM Current (A)
Experiment	688 / 887	9.58	8.67
Simulation	681.6 / 810.2	5.94	7.30

Table 19. Filter with three-phase inductor at 5Hz

60 Hz			
	Vsend/Vrec (V)	Motor Phase Current peak (A)	CM Current (A)
Experiment	700 / 863	11.2	1.7
Simulation	680.0 / 807.9	8.69	1.12

Table 20. Filter with three-phase inductor at 60 Hz with jumpers out

45Hz			
	Vsend/Vrec (V)	Motor Phase Current peak (A)	CM Current (A)
Experiment	700 / 875	11.0	1.7
Simulation	680.0 /806.4	8.11	1.45

Table 21. Filter with three-phase inductor at 45 Hz with jumpers out

5Hz			
	Vsend/Vrec (V)	Motor Phase Current peak (A)	CM Current (A)
Experiment	688 / 898	11.8	2.62
Simulation	685.3 / 809.0	4.62	2.47

Table 22. Filter with three-phase inductor at 5 Hz with jumpers out

Chapter 5: Conclusions and Future Work

In long motor leads application, both the high DM motor voltage and the CM currents create performance and reliability issues. This problem is more pronounced in low power AC drives. Several output filters have been proposed in an attempt to mitigate these effects, but each of these filters has a downside. In this work, two filters that are used by Rockwell Automation were taken into consideration for developing a model to use in simulation tool. The models have shown to reduce the reflective wave problem, CM current and line charging currents. Experimental and simulation results have been provided to compare the models with the existing filters. The results clearly show that the filter model addresses the main issues affecting low power AC drives: reflective wave, CM current and high peak cable charging currents.

Future work will need to be done to address developing a test fixture to measure the saturation characteristics of different types of inductors used in AC drives. This fixture must have the capability to measure DM inductance in the presence of adjustable CM excitation and vice-versa. It must not only demonstrate the usability of the model to typical drive system applications, such as reflected wave, phased current and common-mode current, but also harmonics and power quality, voltage dip and recovery transients.

REFERENCES

[1] Amick, C., Avery, P., & Amer, Y. (2016, February 5). The ABCs (and 1-2-3s) of variable frequency drives. Retrieved from http://machinedesign.com/motorsdrives/abcs-and-1-2-3s-variable-frequency-drives

[2] Rashid, M. H. (2011). *Power electronics handbook: Devices, circuits, and applications* (3rd ed.). Amsterdam, Netherlands: Elsevier/BH.

[3] Bossche, A., & Valchev, V. (2005). *Inductors and transformers for power electronics*. Boca Raton, FL: Taylor & Francis.

[4] TCI, LLC. (n.d.). KDR Line Reactor. Retrieved from http://www.transcoil.com/Products/KDR-Line-Reactor.htm

[5] Streicher, J. T. (n.d.). *Line reactors and AC drives*. Retrieved from Rockwell Automation website: http://literature.rockwellautomation.com/idc/groups/literature/documents/wp/drives-wp016_-en-p.pdf

[6] Eaton Corporation. (2016). *AC line reactors vs DC link chokes* (Application Note AP042003EN). Retrieved from http://www.eaton.com/ecm/idcplg?IdcService=GET_FILE&allowInterrupt=1&RevisionSelectionMethod=LatestReleased&Rendition=Primary&dDocName=AP042003EN

[7] Tallam, R. M., Skibinski, G. L., Shudarek, T. A., & Lukaszewski, R. A. (2011). Integrated differential-mode and common-mode filter to mitigate the effects of long motor leads on AC drives. *IEEE Transactions on Industry Applications*, *47*(5), 2075-2083. doi:10.1109/tia.2011.2161431

[8] Skibinski, G., Dahl, D., Pierce, K., Freed, R., & Gilbert, D. (1998). Installation considerations for multi-motor AC drives and filters used in metal industry applications. *Conference Record of 1998 IEEE Industry Applications Conference. Thirty-Third IAS Annual Meeting (Cat. No.98CH36242)*. doi:10.1109/ias.1998.730131

[9] Lewis-Rzeszutek, H. L., Tallam, R. M., Phukan, R., Solveson, M., & Clancy, T. (2016). Simulation of cable charging current and its effects on operation of low power AC drives. *2016 IEEE Energy Conversion Congress and Exposition (ECCE)*. doi:10.1109/ecce.2016.7855434

[10] Rockwell Automation. (2002). *Wiring and grounding guidelines for pulse width modulated (PWM) AC drives* (Publication DRIVES-IN001A-EN-P). Retrieved from Allen-Bradley Corporation website: http://escventura.com/manuals/ab_VSDWiringGuidelines_rg.pdf

[11] Gönen, T. (2014). *Electric power transmission system engineering analysis and design*. Boca Raton, FL: CRC Press, Taylor & Francis Group.

[12] Lee, Y. (2013). *Introduction to engineering electromagnetics*. Berlin, Germany: Springer.

[13] Rockwell Automation. (2015). *1321 power conditioning products* (Publication No. 1321-TD001P-EN-P). Retrieved from Allen-Bradley Corporation website: http://literature.rockwellautomation.com/idc/groups/literature/documents/td/1321-td001_-en-p.pdf

[14] Von Jouanne, A., & Enjeti, P. (1997). Design considerations for an inverter output filter to mitigate the effects of long motor leads in ASD applications. *IEEE Transactions on Industry Applications, 33*(5), 1138-1145. doi:10.1109/28.633789

[15] Osthold, R. (2009). Innovative output filters for frequency converters. In *13th European Conference on Power Electronics and Applications*. Retrieved from http://ieeexplore.ieee.org/document/5279093/.

[16] Rendusara, D., & Enjeti, P. (1997). New inverter output filter configuration reduces common mode and differential mode dv/dt at the motor terminals in PWM drive systems. *IEEE Power Electronics Specialists Conference*, *2*. doi:10.1109/pesc.1997.616929

[17] Habetler, T., Naik, R., & Nondahl, T. (1999). Design and implementation of an inverter output LC filter used for dv/dt reduction. *Fourteenth Annual Applied Power Electronics Conference and Exposition. 1999 Conference Proceedings (Cat. No.99CH36285), 2*. doi:10.1109/apec.1999.750532

[18] Skibinski, G. L., & Nielsen, H. B. (1999). *Apparatus for eliminating motor voltage reflections and reducing EMI currents* (U.S. Patent 5 990 654).

[19] Singh, Y. (2011). *Electromagnetic field theory*. Noida, India: Pearson Education.

[20] Chaturvedi, P. K., Jain, S., & Agrawal, P. (2008). *National Power Systems Conference*. Bombay, India: Indian Institute of Technology.

[21] Hartman, C. (n.d.). *VFD theory - Power Quality Seminar Series* [PowerPoint]. Retrieved from http://efcnetwork.org/documents/2013/09/ut_em3_variablefreqdrivetheory.pdf

[22] Pulse - A Technitrol Company. (1999). *Understanding common mode noise* (Publication No. G019.A). Retrieved from http://www.pulseelectronics.com/wp-content/uploads/2016/12/G019.pdf.

[23] United States Naval Academy, & Purdue University School of Electrical and Computer Engineering. (2007). *GOSET for use with MATLAB* (Manual Version 2.3). Retrieved from https://engineering.purdue.edu/~sudhoff/Software%20Distribution/GOSET%202.3%20manual.pdf